Nuclear Safety Research

BIENNIAL SCIENTIFIC REPORT 2007-2008 | Volume 3

Forschungszentrum
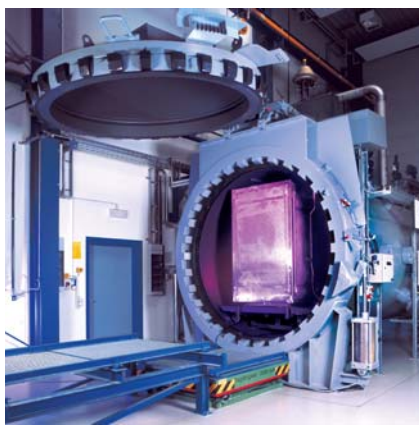**Dresden** Rossendorf

In addition to the Biennial Scientific Reports, the Annual Online Report of the FZD, with research and other highlights of the past year, is available under: www.fzd.de/online-report
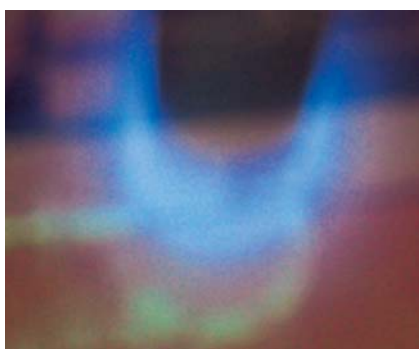
Content

FOCUS

FACILITIES

RESEARCH

FACTS & FIGURES

Preface

Roland Sauerbrey
Scientific Director

The mission of the Forschungszentrum Dresden-Rossendorf (FZD) is excellence in long-term research in socially important issues like energy, health, and advanced material technologies. In strategic collaborations with partners from research and industry the FZD contributes to solve major challenges of modern society. Scientific work at the research center focuses on three questions:

- ◆ How does matter behave in strong fields and at small dimensions?
- ◆ How can cancerous tumors be identified in the early stages and treated effectively?
- ◆ How can the public and the environment be protected from technical risks?

Corresponding to these questions, the Forschungszentrum Dresden-Rossendorf pursues the three program topics "Advanced Materials Research", "Cancer Research", and "Nuclear Safety Research". This Biennial Scientific Report highlights the scientific achievements of the "Nuclear Safety Research" program, covering the years 2007 and 2008. The first part introduces the overall focus of the program as well as the large-scale facilities that are used for research, and the second part consists of eleven articles highlighting research projects that were conducted by scientists of the following institutes:

- ◆ Safety Research
- ◆ Radiochemistry
- ◆ Radiation Physics

In 2007, the FZD was evaluated by the German Council of Science and Humanities (Wissenschaftsrat). In its final evaluation report, published in July 2008, the Council unanimously recommended that the FZD – a Leibniz institution – should become a member of the Helmholtz Association. The report emphasizes: "Since the last evaluation by the German Council of Science and Humanities, the FZD has continuously worked on long-term and highly complex research topics, thus expanding its scientific profile towards a major research center. This top-level research on a strategic and long-term basis in politically and socially important issues suggests an increased financial commitment of the Federal Republic of Germany."

To highlight a few noteworthy events in 2007 and 2008, one must mention the magneto-hydrodynamic (MHD) project of the FZD, which forms a major part of the Collaborative Research Center (SFB) 609 "Electromagnetic flow control in metallurgy, crystal growth, and electrochemistry". The German Science Foundation (DFG) decided in autumn 2008 to prolong the funding for another four years. Moreover, Dr. Frank Stefani, member of the MHD group, and Prof. Günther Rüdiger (Astrophysikalisches Institut Potsdam, AIP) earned the highly prestigious "Society needs Science 2008" award of the "Stifterverband für die deutsche Wissenschaft" for the first experimental demonstration of the magneto-rotational instability. The PROMISE experiment (Potsdam Rossendorf Magnetic InStability Experiment) was conducted in close collaboration between FZD and AIP.

A new focus at the Institute of Radiochemistry, which has been conducting research on actinides, like uranium, for many years, is the interaction of actinides with the bio-system on the cell or even molecular level. Because of the Institute's unique position for uranium and transuranium chemistry in biological systems in Germany, it is a valued partner institution in almost all related research
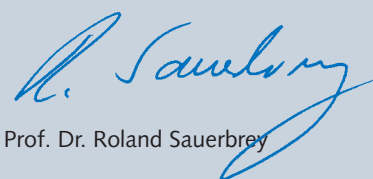
projects in Europe. Within the EU program ACTINET - "Network of Excellence for Actinide Sciences", for example, the radiochemistry station of the Rossendorf Beamline at the ESRF in Grenoble provides about one-third of its beam-time to mainly young researchers allowing them to gain hands-on experience as part of their training.

Research on transmutation is a newly established issue of the Institutes of Safety Research and Radiation Physics. The neutron source needed for the experiments was commissioned towards the end of 2007. The orientation towards research on the safety of Generation IV reactors and of transmutation facilities is a common aim of the FZD Institutes of Radiation Physics and Safety Research, together with the Institute for Energy Management, and for Nuclear and Particle Physics, of the Technische Universität Dresden.

To strengthen the international visibility of the FZD in the scientific community, the FZD served as the local organizer of the IEEE Meetings "Medical Imaging Conference (MIC)" and "Nuclear Science Symposium (NSS)". The 2008 IEEE-NSS-MIC Conference took place in Dresden from October 19 to 25, and scientists of the Nuclear Safety Research program were actively engaged in it. Just to give one example, Dr. Uwe Hampel presented the world record for ultra high-speed electron beam X-ray tomography. It is noteworthy that his conference paper received the highest ranking by the responsible MIC committee. All in all, the Dresden IEEE Conference attracted more than 2,700 participants, thus being the largest IEEE-NSS-MIC Conference ever. We are very grateful to the German Science Foundation (DFG) and the Saxon State Ministry of Higher Education, Research and the Arts (SMWK) for their essential contributions of funding for the Conference.

The success of a research institution strongly depends on the motivation and dedication of talented young scientists. The FZD has put a lot of effort into attracting junior scientists from Germany and abroad. Our six institutes strive for excellent working conditions and support of their staff, the FZD as a whole offers Ph.D. seminars to about 120 doctoral students, a tenure track program for out-standing postdoctoral staff, special workshops for young scientists such as communication to the media, presentation in English, training for young science managers, etc. The FZD supports high-level training as well for its technical staff and its almost 60 trainees. In 2008, the FZD received the "Audit Beruf und Familie" (Career and Family Certificate) from the Hertie Foundation, underlining the particular importance attached to the healthy balance of family and career at the FZD.

Finally, this preface gives me the opportunity to thank our funding institutions, the Saxon State Ministry of Higher Education, Research and the Arts (SMWK) and the Federal Ministry of Education and Research (BMBF), for their continued support, our national and international scientific coop-eration partners for many successful joint research endeavors, and the entire staff of the FZD for their dedicated work.

Prof. Dr. Roland Sauerbrey
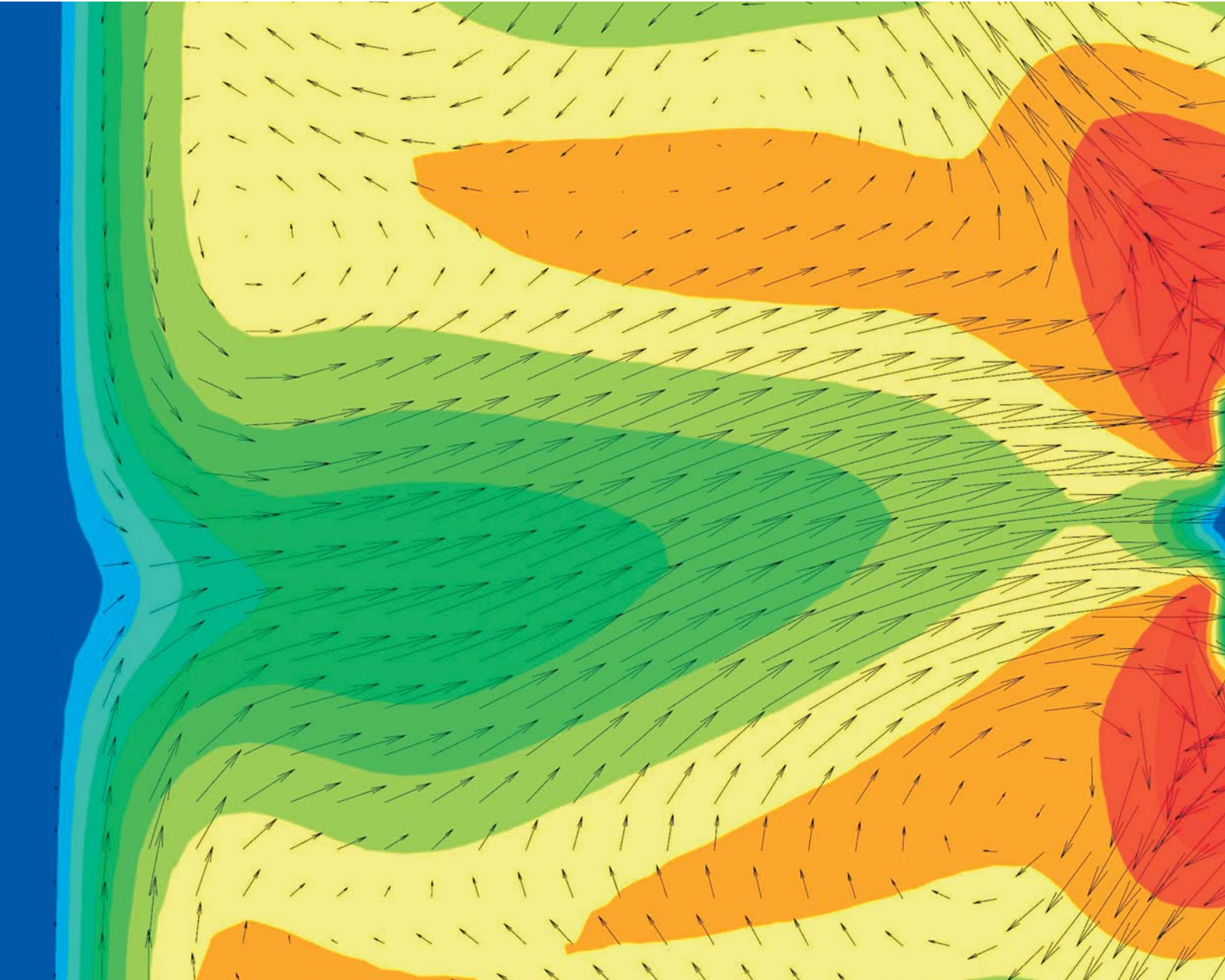
Nuclear Safety Research program

at the Forschungszentrum Dresden-Rossendorf

Frank-Peter Weiss, Gert Bernhard,
Thomas E. Cowan

This program is focused on the protection of the public and the environment against industrial hazards. For this purpose, our research mainly aims at assessing and enhancing the safety, efficiency, and sustainability of nuclear reactors of current and future designs as well as of the geological disposal of radioactive waste. It is the particular goal to evaluate and minimize the risks related to the nuclear fuel cycle. This includes the relics of former uranium mining, power generation in nuclear reactors, as well as the reduction and the final geological disposal of radioactive waste. Many of the scientific methods and tools used in nuclear engineering are also successfully adapted to non-nuclear fields, for example to optimize industrial processes by customized flow control.

The Nuclear Safety Research program is implemented by the Institute of Radiochemistry, the Institute of Radiation Physics, and the Institute of Safety Research. It includes research in the fields of radioecology, reactor safety, neutron physics, and thermal fluid dynamics. Whereas radioecology focuses on the identification of the chemical interaction and the mobility of radionuclides, especially of actinides, in the geo- and the bio-spheres, our research in neutron physics aims at improved measurement of the neutron-induced transmutation of radionuclides in order to minimize long-lived radioactive waste. The reactor safety research is directed towards the development of physical simulation tools used for nuclear reactor accident analysis and the description of ageing phenomena in irradiated reactor construction materials.
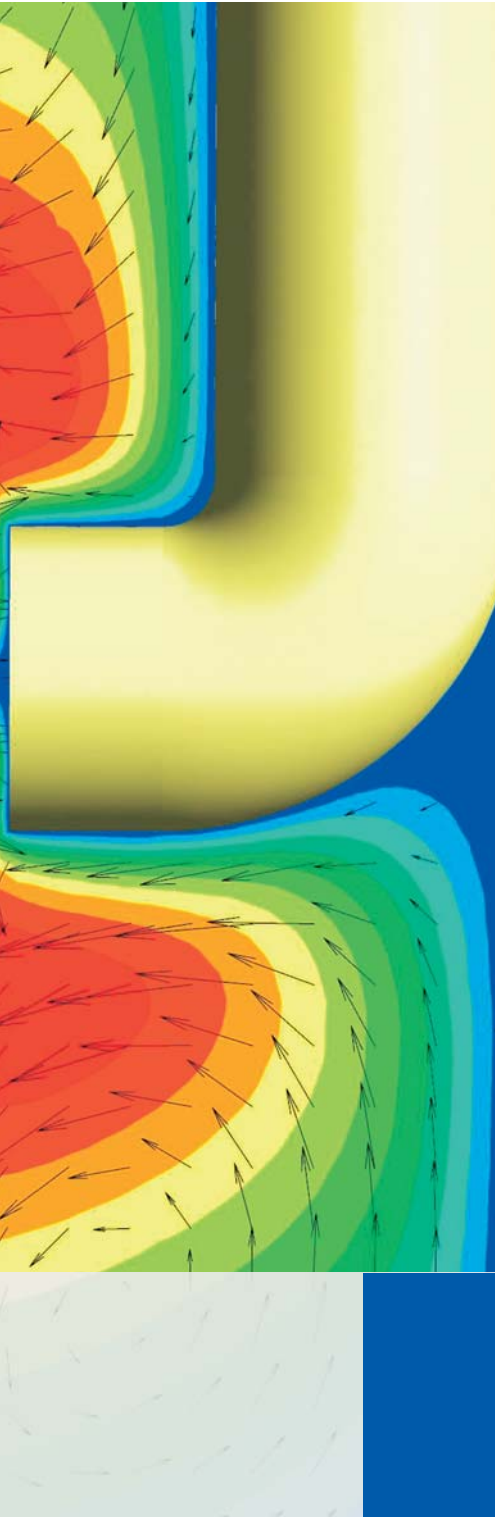
Complementing this, in our research on thermal fluid dynamics we study transient multi-phase flows and magneto-hydrodynamic (MHD) phenomena to provide the basis for advanced process simulation. The development and validation of tools for process simulation, accident analysis, and long-term safety assessment of the disposal of radio-active waste, with the emphasis on thermo and fluid dynamic computation methods, constitute the framework for our research.

The Nuclear Safety Research program is supported by large-scale experimental user facilities operated by the FZD such as the Radiation Source ELBE, the Rossendorf Beamline ROBL at the ESRF in Grenoble, and the Transient Two-Phase Flow Test Facility (TOPFLOW). In addition, close collaborations exist with the other research programs of the FZD, which are devoted to Cancer Research and Advanced Materials Research. Within the framework of the latter the MHD group deals with the optimization of flows in crystal growth and metallurgy. Further collaborations are related for example to the development of biological metal templates with modified magnetic properties for the Dresden High Magnetic Field Laboratory (HLD). In the fields of irradiation-induced materials and ageing and surface layer characterization, we benefit considerably from the expertise at the Institute of Ion Beam Physics and Materials Research. Moreover, we contribute to the development of new macromolecules for nuclear medicine by our competence in laser spectroscopy.

The reactor safety and radioecology research is integrated in the German Alliances for Competence in Nuclear Technology (Kompetenzverbund Kerntechnik), and for Competence in Radiation Research (Kompetenzverbund Strahlenforschung).

TOPFLOW Facility:
Looking through impenetrable walls

Uwe Hampel, Dirk Lucas, Helmar Carl

The multi-purpose thermal hydraulic test facility TOPFLOW (Transient Two-Phase Flow Test Facility) is one of the major research facilities at the FZD, and is designed for studying thermal hydraulic phenomena of steam-water two-phase flows at high pressures and temperatures (Fig. 1). It is devoted to basic and applied research on two-phase flow phenomena, which play a key role in many industrial processes such as in nuclear power plants, chemical reactors, and oil processing [1]. TOPFLOW, with its maximum steam power generation capacity of 4 MW, allows performing steam-water two-phase

flow experiments at industrially relevant pressures of up to 7 MPa and saturation temperatures of 286 °C. Current projects focus on computational fluid dynamics (CFD) code validation for two-phase flows, experimental investigation of nuclear reactor safety issues such as pressurized thermal shock scenarios, and test of industrial plant components like valves and nozzles. TOPFLOW is the reference test facility of the German Alliance for CFD in nuclear reactor safety.

One of the distinctive features of the TOPFLOW facility is the availability of advanced two-phase flow instrumentation. A key instrument is the wire mesh sensor [2],

which was developed at the FZD and has become an important two-phase flow measurement tool at TOPFLOW and in many other facilities worldwide. The sensor (Fig. 3) allows visualization of the flow structure of complex two-phase flows with high spatial (2 mm) and temporal resolution (up to 10,000 images per second). Recently, a new technique called ultra fast electron beam X-ray tomography has been installed at TOPFLOW which allows non-invasive flow measurement with similar performance. Such advanced measurement technology combined with standard industrial and scientific flow instrumentation, for example high speed and IR cameras, needle probes for void and flow

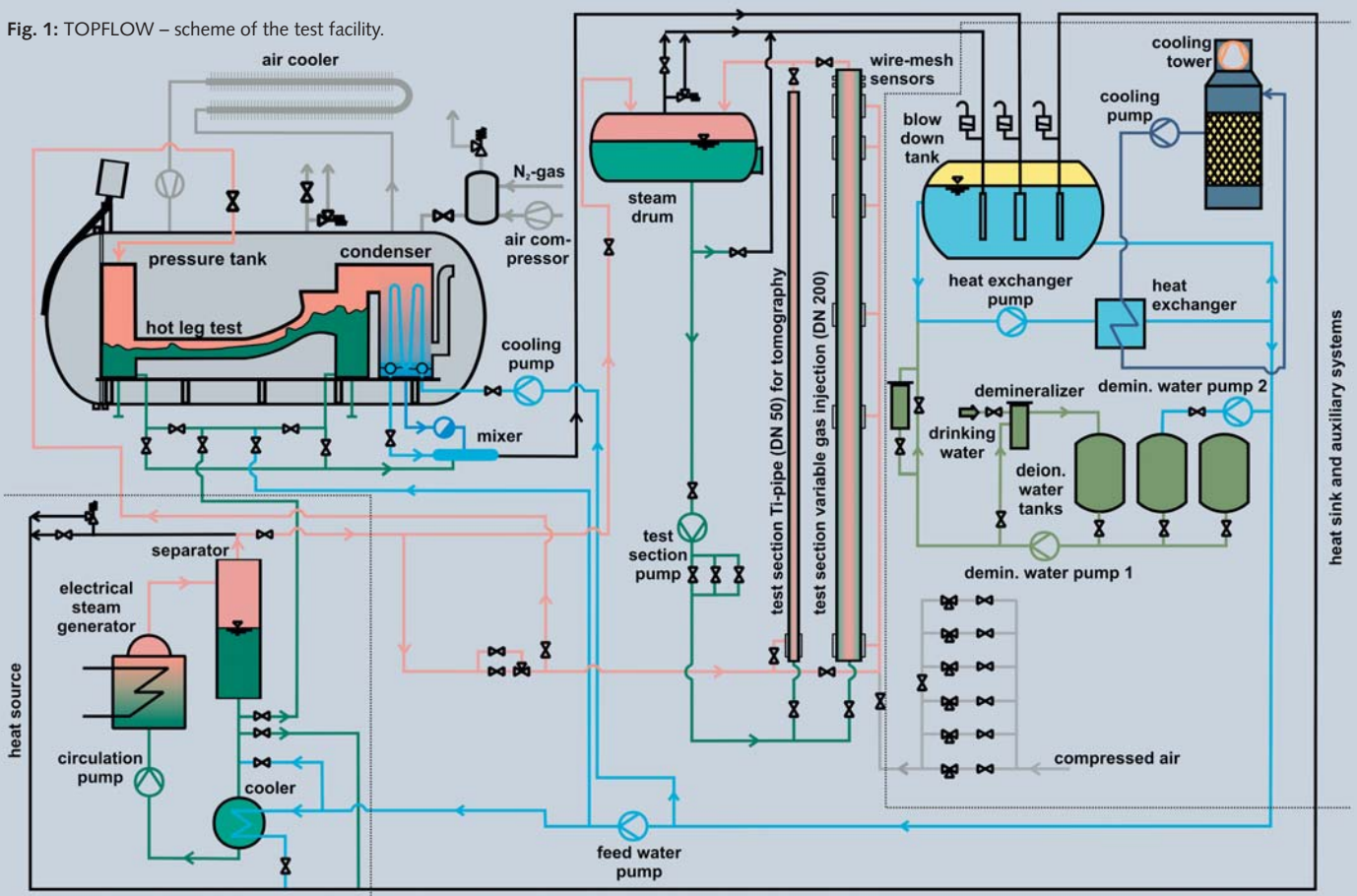**Fig. 1:** TOPFLOW – scheme of the test facility.

Fig. 2: TOPFLOW pressurized vessel for the operation of test sections and components in pressure equilibrium with the vessel atmosphere. This technology allows the application of optical and IR measurement techniques at pressures up to 50 bars.

temperature measurement, and gamma ray densitometry, allow the study of flow phenomena with unprecedented disclosure of flow details, such as phase and interfacial area distribution.

Another unique feature of TOPFLOW is a large pressure chamber (Fig. 2) which serves as a pressurized laboratory for experiments in complex flow domain geometries. The latter allows operating

thermal hydraulic test rigs of up to 7 m length and 2 m height in pressure equilibrium which enables optical and infrared flow observation through thin walls or glass windows.

Currently, the TOPFLOW facility is used in the framework of three major projects. The first of them is devoted to CFD validation and model development for applications in nuclear reactor safety [3]. It is funded by the German Federal Ministry of Industry (BMWi). In the second project, Pressurized Thermal Shock (PTS) phenomena are studied in detail, as they represent a crucial reactor safety issue for aged reactor pressure vessels during emergency core cooling in a loss-of-coolant scenario. The project is a collaboration of seven industrial and scientific partners: Commissariat à l'Energie Atomique (CEA) France, Electricité de France (EdF), AREVA NP France, Institut de Radioprotection et de Sûreté Nucléaire (IRSN) France, Paul Scherrer Institute (PSI) Switzerland, ETH Zürich, Switzerland, and FZD. The third project, which is conducted in cooperation with Nederlandse Aradolinie Maatschappij B. V. (NAM) Netherlands, aims at the investigation of critical flow conditions in a steam nozzle.

Beyond these projects, there are an additional 8 institutions worldwide which make use of TOPFLOW experimental data in the framework of bilateral collaborations.

References

[1] *Gas/liquid flow in large risers*, N.K. Omebere-Iyari, B.J. Azzopardi, D. Lucas, M. Beyer, H.-M. Prasser, International Journal of Multi-Phase Flow 34, 461 – 476 (2008)

[2 *Evolution of the structure of a gas-liquid two-phase flow in a large vertical pipe*, H.-M. Prasser, M. Beyer, H. Carl, S. Gregor, D. Lucas, H. Pietruske, P. Schütz, F.-P. Weiss, Nuclear Engineering and Design 237, 1848 – 1861 (2007)

[3] *Gas-liquid flow around an obstacle in a vertical pipe*, H.-M. Prasser, M. Beyer, T. Frank, S. Al Issa, H. Carl, H. Pietruske, P. Schütz, Nuclear Engineering and Design 238, 1802 – 1819 (2008)

Project partners
· Commissariat à l'Energie Atomique, France
· Electricité de France, France
· Institut de Radioprotection et de Sûreté Nucléaire, France
· AREVA NP, France
· Paul Scherrer Institute, Switzerland
· ETH Zürich, Switzerland
· Nederlandse Aradolinie Maatschappij B. V., Netherlands
· Université Catholique de Louvain, Belgium
· Computational Dynamics Limited, UK
· University of Nottingham, School of Chemical, Environmental and Mining Engineering, UK
· Norwegian University of Science and Technology, Trondheim, Norway
· Idaho National Lab, USA
· Rensselaer Polytechnic Institute, USA
· Gadjah Mada University, Yogyakarta, Indonesia
· Royal Melbourne Institute of Technology, Australia
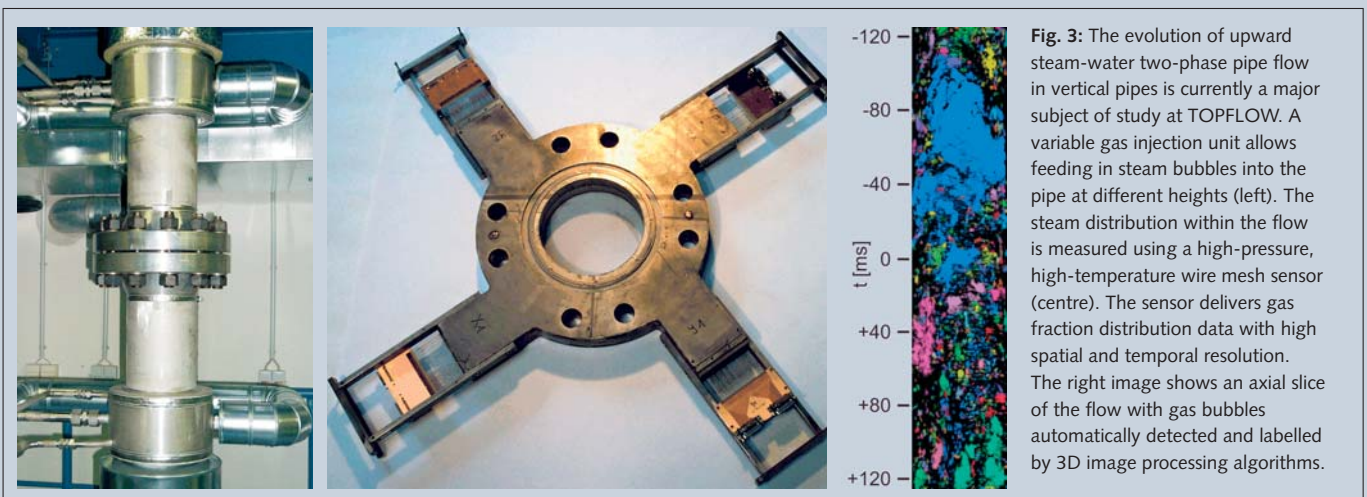
Fig. 3: The evolution of upward steam-water two-phase pipe flow in vertical pipes is currently a major subject of study at TOPFLOW. A variable gas injection unit allows feeding in steam bubbles into the pipe at different heights (left). The steam distribution within the flow is measured using a high-pressure, high-temperature wire mesh sensor (centre). The sensor delivers gas fraction distribution data with high spatial and temporal resolution. The right image shows an axial slice of the flow with gas bubbles automatically detected and labelled by 3D image processing algorithms.

The Rossendorf Beamline (ROBL)

Selenium-79 – a radionuclide highly mobile in the environment?

Andreas C. Scheinost

The Rossendorf Beamline (ROBL) at the European Synchrotron Radiation Facility (ESRF) in Grenoble, France, offers the unique opportunity to investigate the chemical state of radionuclides at very low concentrations (down to a few parts per million). The beamline is therefore ideally suited for fundamental research required to assess the safe disposal of nuclear waste, which is one of the great challenges of society in the 21st century.

Current deep-geological disposal concepts are considered to be highly efficient in retaining cationic (positively charged) radionuclide species, which include fission products like cesium and strontium, as well as soluble actinide species. Anionic (negatively charged) radionuclide species, however, may pass through these barriers easily since anion adsorbing mineral surfaces (mostly Fe(III) oxides) are scarce in the oxygen-depleted conditions of deep geological formations. Especially the radioisotope selenium-79 is of high concern because, firstly, it forms soluble anionic species at three of its four oxidation states (-II, IV and VI), and, secondly, it has a very long half-life of one million years. Consequently, several national risk assessment reports have predicted that selenium-79 will dominate the radioactive dose released from nuclear waste repositories into the biosphere for one million years into the future after closure.

Yet selenium may not only occur as soluble anions, but also as elemental Se and metal selenides (Se oxidation states 0 and -II), solids with extremely low solubility. If Se(IV) or Se(VI) were reduced to these lower oxidation states, then these insoluble solids may precipitate out of solution, thereby preventing selenium migration. In fact, anoxic waste repositories are rich in Fe(0) and Fe(II)-containing surfaces, which could promote selenium reduction by a coupled redox reaction (Se is reduced, Fe is oxidized). Although this process is predicted to proceed based on thermodynamics, it may be prevented by slow reduction kinetics. Earlier attempts to investigate the reduction process experimentally were hampered by the difficulty to maintain strictly anoxic conditions during sample preparation and the selenium speciation steps, which commonly have to be performed at various lab facilities, as well as by the slow redox kinetics.
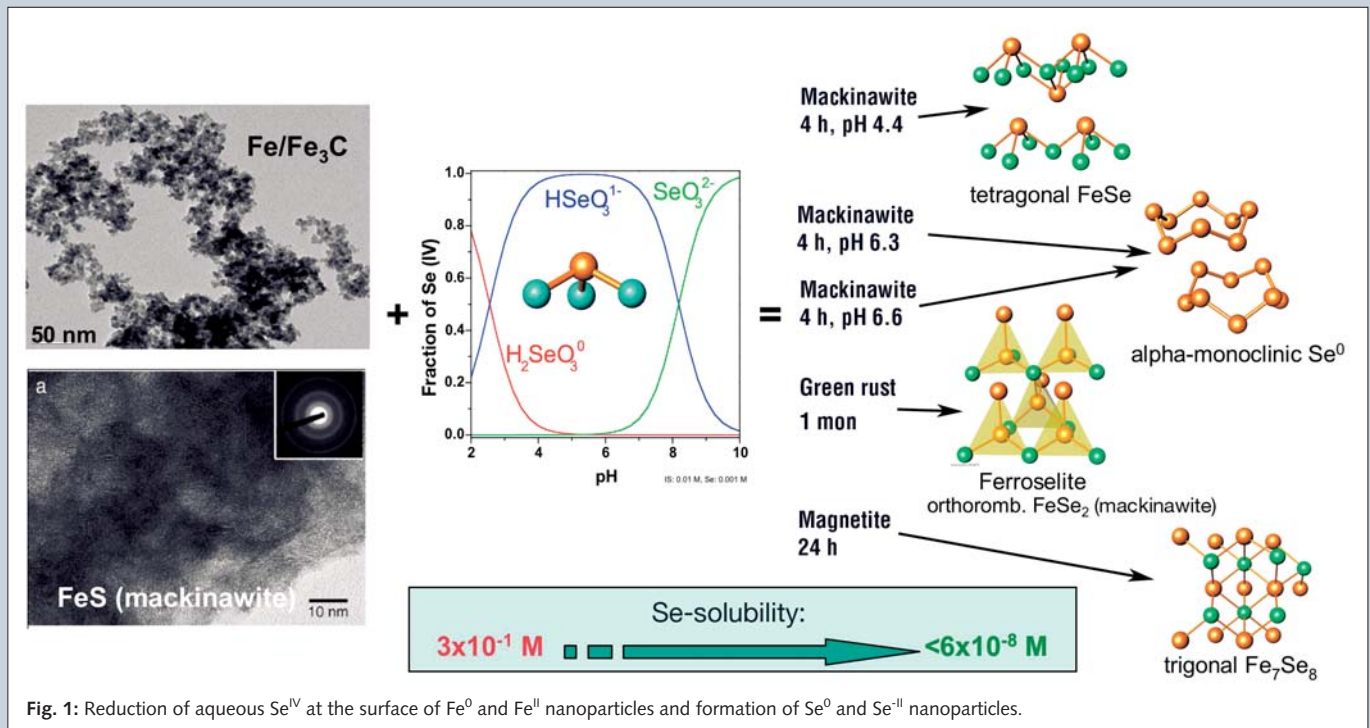

Fig. 1: Reduction of aqueous Se^{IV} at the surface of Fe^{0} and Fe^{II} nanoparticles and formation of Se^{0} and Se^{-II} nanoparticles.

A recent collaboration between the French National Center for Scientific Research (CNRS), the universities of Grenoble, Bordeaux and Le Mans in France, Umea in Sweden and the FZD, supported by ACTINET – European Network of Excellence, has now finally brought a major breakthrough by bringing together an array of techniques, including X-ray Absorption Spectroscopy (XAS) at the Rossendorf Beamline of the ESRF, High-Energy X-ray Scattering (HEXS) at the ESRF Beamline ID-15B, cryogenic X-ray PhotoSpectroscopy (XPS) at the University of Umea (Sweden), Moessbauer spectroscopy at the University of Maine (France), and by ensuring an oxygen-free transport chain from the anoxic glove box at the University of Grenoble to the spectroscopy facilities.

The selenite reduction mechanisms were investigated in a range of iron(II) systems representing the different barriers in a typical nuclear waste repository: (1) nanoparticulate zerovalent iron, green rust, and magnetite which occur at the surface of corroding steel containers for spent nuclear fuel; (2) the clay mineral montmorillonite with adsorbed or structural Fe(II) which occurs in the bentonite backfill surrounding the waste containers; (3) mackinawite, siderite, and magnetite which are typical Fe(II)-minerals ubiquitous in geological bedrock and aquifer sediments.

X-ray Absorption Near-Edge Structure (XANES) spectroscopy was used to follow the redox state of selenium over time. In contrast to the otherwise slow reduction kinetics of selenium, selenite reduction was completed within 24 hours (sometimes within 10 to 30 min) in the presence of nanoparticulate zero-valent iron, magnetite, green rust, and mackinawite (Fig. 1), in line with a fast electron transfer rate at the surfaces of these metallic or semiconducting solids. In contrast, the large band-gap of the Fe(II)-carbonate siderite and of Fe(II)-montmorillonite resulted in much slower reaction kinetics, where even after reaction times of 1 to 2 months only partial selenite reduction was obtained.

In the Fe(II)-montmorillonite system, we were able to follow the oxidation state of Fe by using Fe-57 Moessbauer spectroscopy (Fig. 2). Even before adding the redox partner Se, 1/4 of Fe(II) was rapidly oxidized within a few minutes. In contrast, Se reduction was slow, with only 3/4 completed within one month. No further Fe(II) oxidation was observed during this time, suggesting that the iron oxidation and selenium reduction reactions are not directly coupled. By combining surface complexation modeling, Density Functional Theory (DFT) quantum chemical calculations and thermodynamics, a complex reaction scheme was elucidated, where Fe^{2+} forms an activated surface complex, followed by oxidation of iron and formation of hydrogen from water. This hydrogen species remains sorbed to the montmorillonite surface and is then later available for Se(IV) reduction.
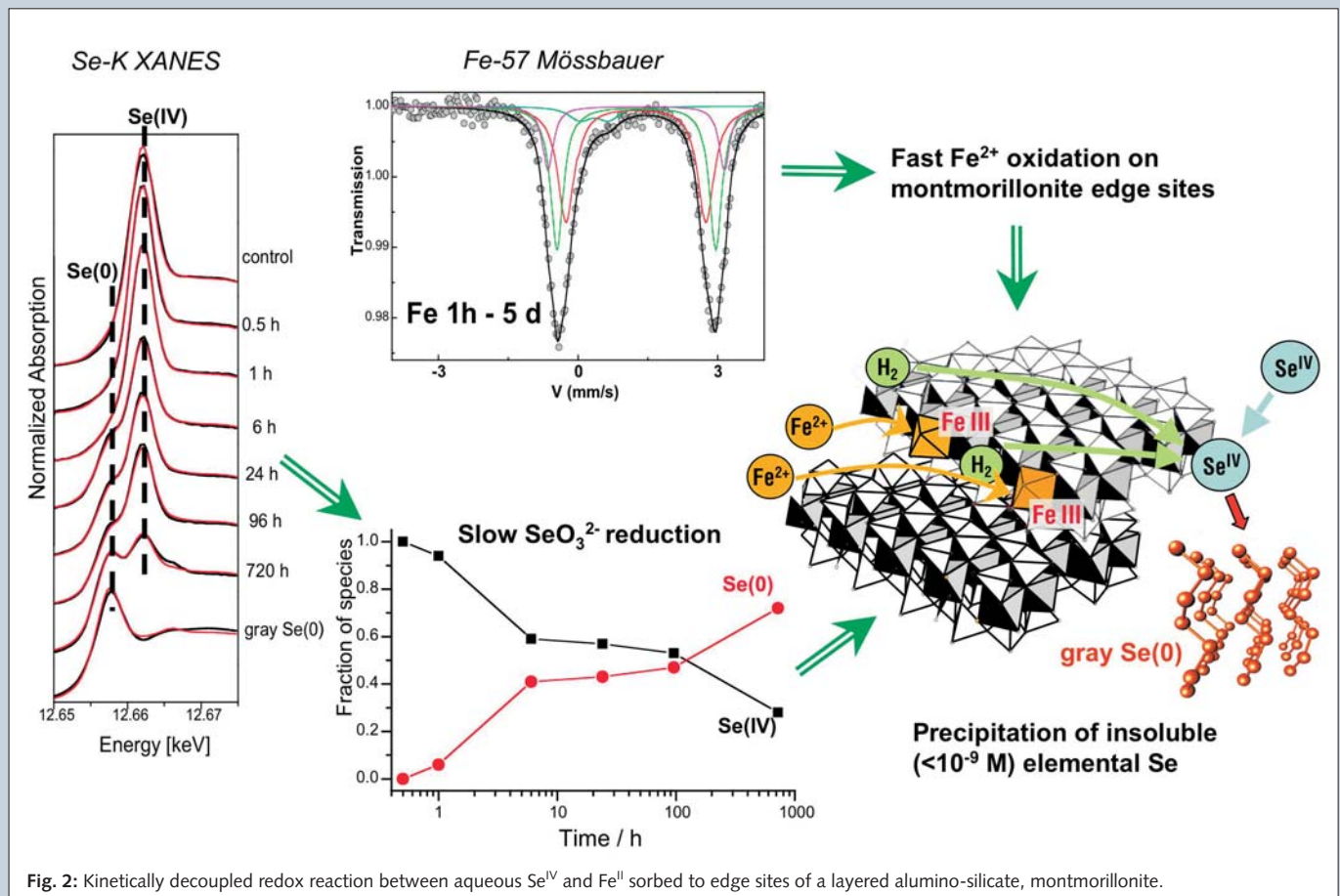

Fig. 2: Kinetically decoupled redox reaction between aqueous Se^{IV} and Fe^{II} sorbed to edge sites of a layered alumino-silicate, montmorillonite.

Using Extended X-ray Absorption Fine-Structure (EXAFS) spectroscopy, we identified a range of amorphous and nanoparticulate reduced Se phases, including red (amorphous) and gray (triclinic) elemental Se, and Fe^{II} selenide phases similar to tetragonal FeSe and Fe_7Se_8. The Fe(II) selenides formed at the surface of magnetite, green rust, and mackinawite, i.e. during rapid Se reduction, while elemental Se formed only during slow Se reduction. This difference could be explained by the concentration of a reduced intermediate species, aqueous HSe^-, which favors formation of Fe^{II} selenides.

Now what about the effect of selenium reduction on selenium concentration in solution? Elemental selenium and iron(II) selenides have an extremely low solubility (in the order of 10^{-9} M). If particle sizes reach the lower nanometer range, however, surface tension may drastically grow, thereby increasing solubility by several orders of magnitude in comparison to larger crystals. This effect was not observed in our experiments. Whenever Se(IV) was completely reduced, Se concentration dropped below the detection limit (about 10^{-8} M) close to the values of bulk minerals.

This low solubility is already an important requirement to keep selenium transport by groundwater in aquifers small. Given the appropriate physico-chemical conditions (low ionic strength and a pH far apart from the point of zero charge of the particles), selenium nanoparticles may form stable colloidal suspensions which are then transported through the pore space of aquifers with a speed even faster than that of a conservative (non-sorbing) solute.

Our investigations showed, however, no tendency of the nanoparticles to detach from the surfaces and to form mobile colloids.

Our research suggests that radioactive selenium will be retained by the steel containers constituting the first confinement for nuclear waste, even if these containers are corroding. The clay backfill surrounding the containers, as well as the Fe^{II} minerals naturally occurring in aquifer sediments, provide further protection of the biosphere from radioactive selenium-79. In conclusion, our study shows for the first time that the risk associated with selenium-79 may be much smaller than previously assumed, providing an important step towards the safe disposal of nuclear waste.

References

[1] *Electron transfer at the mineral/water interface: Selenium reduction by ferrous iron sorbed on clay*, L. Charlet, A.C. Scheinost, C. Tournassat, J.M. Greneche, A. Géhin, A. Fernández-Martínez, S. Coudert, D. Tisserand, J. Brendle, Geochimica et Cosmochimica Acta 71(23), 5731 – 5749 (2007)

[2] *Selenite reduction by mackinawite, magnetite and siderite: XAS characterization of nanosized redox products*, A.C. Scheinost, L. Charlet, Environmental Science & Technology 42, 1984 – 1989 (2008)

[3] *X-ray absorption and photoelectron spectroscopy investigation of selenite reduction by FeII-bearing minerals*, A.C. Scheinost, R. Kirsch, D. Banerjee, A. Fernandez-Martinez, H. Zaenker, H. Funke, L. Charlet, Journal of Contaminant Hydrology 102, 228 – 245 (2008)

[4] *Immobilization of selenite on Fe_3O_4 and Fe/FeC_3 ultrasmall particles*, R.L.d.A. Loyo, S.I. Nikitenko, A.C. Scheinost, M. Simonoff, Environmental Science & Technology 42(7), 2451 – 2456 (2008)

[5] *Synthesis of a Se^0/calcite composite using hydrothermal carbonation of $Ca(OH)_2$ coupled to a complex selenocystine fragmentation*, G. Montes-Hernandez, A. Fernández-Martínez, L. Charlet, F. Renard, A.C. Scheinost, M. Bueno, Crystal Growth & Design 8(7), 2497 – 2504 (2008)
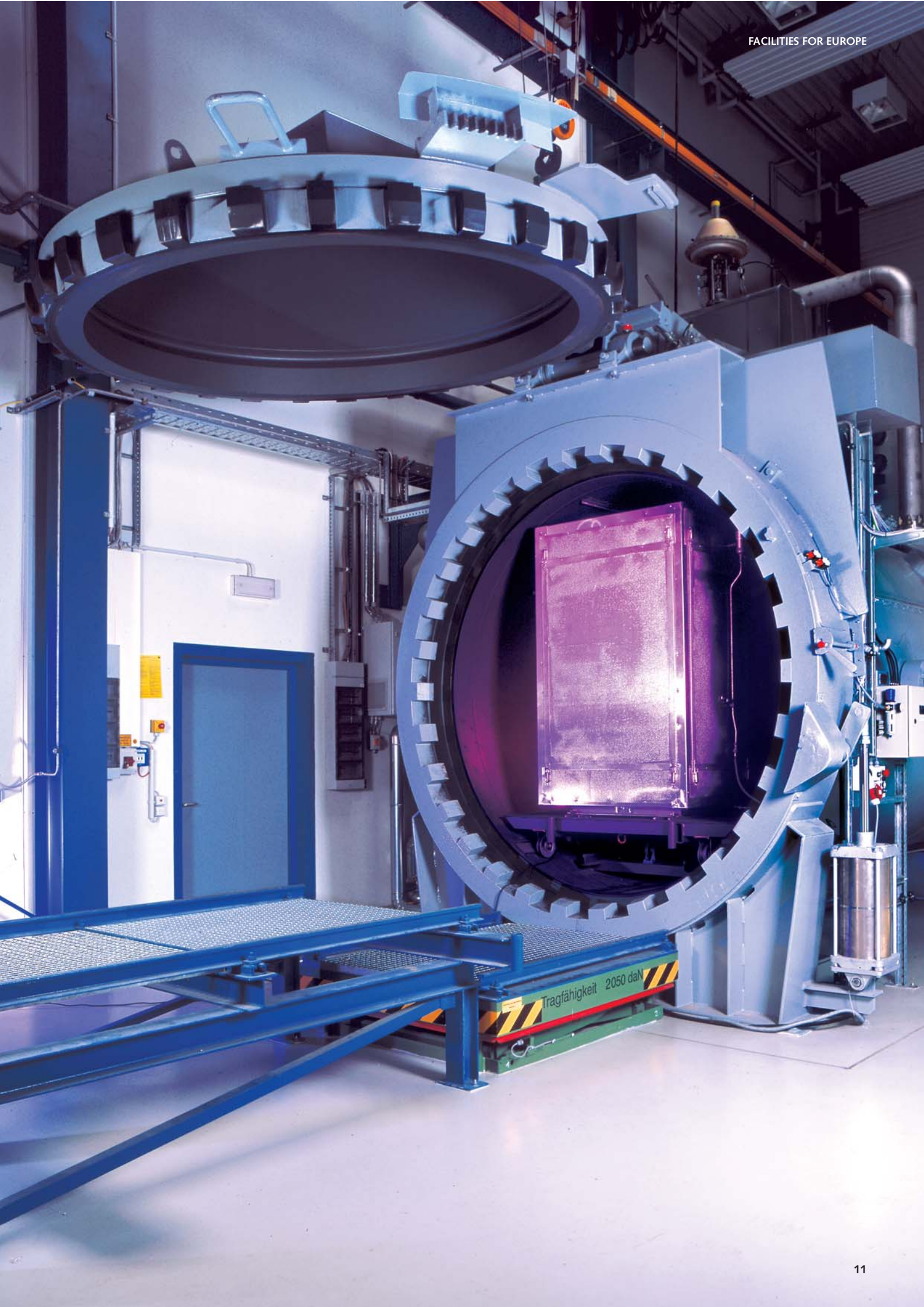
Research

Fast neutrons for transmutation of nuclear waste

Arnd R. Junghans

The partitioning of nuclear waste and transmutation of long-lived isotopes to nuclides with shorter lifetime is an important topic in international research to provide sustainable sources of energy which are free of greenhouse gas emissions (see Fig. 1). Different designs involving critical reactors or sub-critical accelerator-driven systems (ADS) are being studied in view of their transmutation capabilities, as well as new concepts to produce less waste via very high burn-up. The Generation IV International Forum (GIF) has selected six nuclear energy

systems for which research and development are ongoing to confirm their viability and to demonstrate their expected performance that includes the objective of producing less waste.

In the considerations for waste reduction, the possible use of fast (i.e. un-moderated) neutrons coming directly from the fission process is of great importance as most of the proposed systems use a fast neutron spectrum. Reliable predictions of the relevant physical processes, and the optimization of the related facilities, depend on the availability of high-quality nuclear data. The data needs have been

investigated by the working party on evaluation co-operation (WPEC) of the OECD Nuclear Energy Agency. Two important research fields were identified to be the inelastic scattering of fast neutrons on structure materials in reactors and transmutation devices, and the neutron-induced fission process of minor actinide nuclei.

The EURATOM framework programs continue to foster European research in the field of nuclear transmutation: The neutron time-of-flight facility nELBE at the For-schungszentrum Dresden-Rossendorf is part of the Integrated Infrastructure Initiative (I3) entitled "European Facilities for Nuclear Data Measurements" (EFNUDAT), which has been created by a consortium of 10 experimental facilities in 7 European countries for nuclear data measurements. Joint Research Activities (JRA) within this I3 include the data acquisition using fast digitizers, quality assurance of nuclear data, and the development of neutron producing target technology.

Photoproduction of neutrons at ELBE
ELBE is the first superconducting electron linear accelerator combined with a neutron time-of-flight facility. Time-of-flight measurements take advantage of a high pulse repetition rate of 100 kHz to 500 kHz. This is nearly a factor of 1000 higher than the pulsed operation at normal-conducting accelerators. The instantaneous neutron and photon flux is lower, which can lead to improved background conditions from the scattered photon flash.

The nELBE neutron time-of-flight facility is now operational for experiments at the ELBE superconducting linear accelerator.
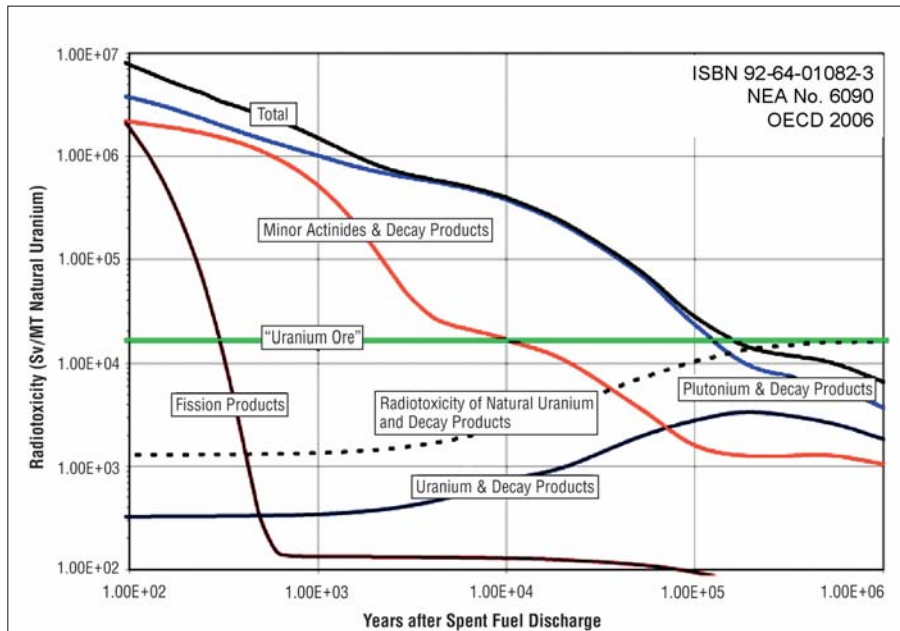
Fig 1: Evolution in time of the radiotoxicity of the waste from a conventional uranium reactor and its components. This graph was prepared by the Nuclear Energy Agency (NEA), a specialized agency within the Organization for Economic Co-operation and Development (OECD). This plot includes effects resulting from a possible incorporation of waste components decaying by α-decay or fission. The radiotoxicity of plutonium and other (minor) actinides decay to the natural level of the uranium ore only after 10 to 100 thousand years, and thus their removal by transmutation is especially important. Source: Physics and Safety of Transmutation Systems – A Status Report, p. 9, OECD 2006

Fast neutrons in the energy range from ~0.1 to 10 MeV are produced by the pulsed electron beam from ELBE impinging on a liquid lead circuit as a radiator. In Fig. 2, the experimental neutron energy spectrum at nELBE is shown in comparison with a neutron spectrum typical of the neutron induced fission of ^{235}U. The energy spectrum measured at nELBE has a very similar shape as the fission spectrum from fast neutrons, demonstrating that the energy range relevant for reactions with fast neutrons in reactor and transmutation systems can be investigated. The short

beam pulses of ~10 ps provide the basis for an excellent time resolution for neutron time-of-flight experiments, giving an energy resolution of about < 1 % at 1 MeV with a short flight path of ~6.5 m. A neutron source strength of ~5 x 10^{10} neutrons per second has been reached, resulting in a neutron intensity on target of ~3 x 10^4 n/(cm^2 s) using an electron bunch charge of 77 pC at 100 kHz pulse repetition rate.

The neutron flux – which determines the statistical accuracy of a cross section measurement carried out in a given time – depends on the primary beam intensity and on the amount of converter target material exposed to the beam in the neutron source. A liquid lead circuit is used to cope with the very high beam power deposition (P ≈ 5 kW/g) and to allow efficient cooling. It was designed and built in a collaborative effort of the FZD institutes of Radiation Physics and of Safety Research [1]. The liquid lead circuit has been operated for more than 800 hours without any significant failures.

Fig 2: Neutron energy spectrum measured at nELBE (red curve) using a ^{235}U fission chamber, an electron beam energy of 25 MeV and a 652 cm neutron flight path. The peaks on the low energy side of the spectrum are due to the fine structure of the dipole strength distribution in the isotopes of the neutron radiator. The blue curve is a neutron spectrum from the fission of 235-U induced by fast neutrons with E_n = 10 MeV, taken from the evaluated nuclear data file ENDF/B-VII.0 (scaled to the measured data).

Experimental setup at nELBE

In two experiments, the inelastic neutron scattering of ^{56}Fe and the total neutron cross section σ_{tot} of ^{181}Ta have been measured. The total neutron cross section has been determined in a transmission experiment in the energy range from 300 keV to 8 MeV. Between 800 keV and 1600 keV only very sparse data existed up till now. The energy resolution obtained at nELBE was 0.7 % at 2 MeV neutron energy. The relative statistical error in the cross section was about 2 % after 33 h of beam time.

Fig. 3: The inelastic neutron scattering experiment from downstream direction. The neutron beam travels through the Barium-Fluoride (BaF$_2$) detector array in the middle of the picture and passes the ^{235}U fission chamber from Physikalisch-Technische Bundesanstalt (PTB) on the right side, to be stopped in a beam dump. The target is located at the center of the BaF$_2$ array, for example a sample of ^{56}Fe, from which neutrons are scattered. Neutrons are detected by plastic scintillation counters on the left side (yellow). The simultaneously emitted photons are measured in the BaF$_2$ array.

The time-of-flight, and thus the neutron energy, is determined with plastic scintillators with a low detection threshold, as shown in Fig. 3. Measurements with a ^{235}U fission chamber from the Physikalisch-Technische Bundesanstalt (PTB) Braunschweig allowed to determine the absolute neutron intensity of the beam. By comparison of data with and without a Cd-shield, an upper limit for the relative thermal neutron flux of less than 8 x 10^{-5} was determined.
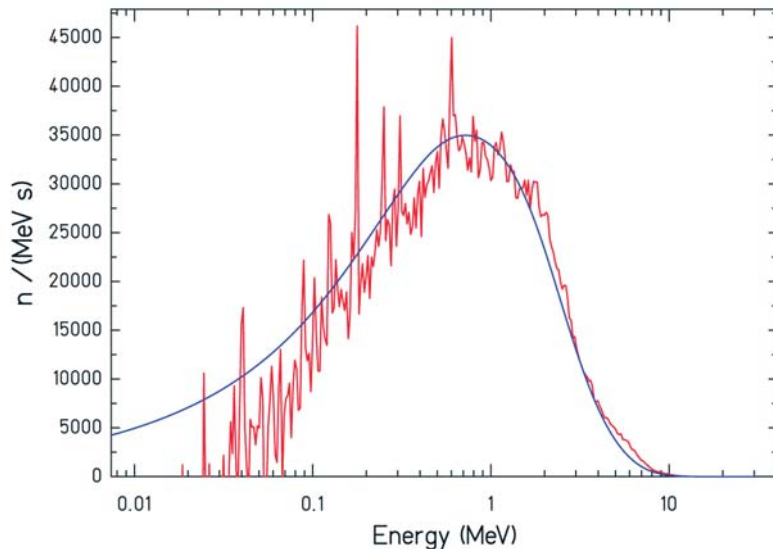
Inelastic neutron scattering is being investigated using a compact 4π-array of BaF_2 scintillators which consist of up to 42 hexagonally shaped crystals (19 cm long by 53 mm diameter, see Fig. 3). By a double time-of-flight measurement, the energy of the incoming neutron and of the scattered neutron can be determined. The scattered neutrons are detected by an array of 5 plastic scintillators (100 cm long by 4.2 cm wide by 1.1 cm thick). By using the photon and neutron detectors in coincidence, inelastic neutron scattering can be identified. Both detector types reach time resolutions below 1 ns, and are thus well suited for a proper time-of-flight tagging. Fig. 4 shows the coincident (incident and scattered) neutron spectrum from the double time-of-flight measurement, in which scattering from the 1st and 2nd excited state can be separated. The experiment also allows to measure the angular distribution of the scattered neutrons.

Fig. 4: Double time-of-flight measurement of the incoming neutron and the scattered neutron from a ^{nat}Fe target. The lines indicate the region where, within the given energy resolution, the 1st up to the 4th excited state of ^{56}Fe should be located.

Outlook

The experimental program to measure inelastic neutron scattering and total neutron cross sections in the fast neutron range from 0.1 to 10 MeV has begun at nELBE. Structural materials that are relevant for nuclear transmutation systems are being investigated currently.

With the higher intensity available with the superconducting radiofrequency (SRF) injector of ELBE, neutron induced fission cross section of actinides can be investigated. Minor actinides will be analyzed in a fission ionization chamber prepared with thin films of the radioactive target material. The radiochemical requirements are stringent: isotopically pure material needs to be used to create homogeneous thin films, with an areal density of typically $100\,mg/cm^2$, to be able to register the fission fragments with good signal to noise ratio. The sample and target preparation for minor actinides is being conducted as part of the joint research activities of the EFNUDAT project as well.

Fig. 5: The nELBE photo-neutron source together with the final section of the electron beam line. The electron beam focused by quadrupole magnets (painted blue) hits the liquid lead inside a cylindrical vacuum chamber, where high-intensity neutron pulses are produced. Afterwards, the beam is stopped in a lead-shielded beam dump. The liquid lead is circulated with an induction pump through a heat exchanger in a thermally insulated and electrically heated circuit.

Reference

[1] *A photo-neutron source for time-of-flight measurements at the radiation source ELBE*, E. Altstadt, C. Beckert, H. Freiesleben, V. Galindo, E. Grosse, A.R. Junghans, J. Klug, B. Naumann, S. Schneider, R. Schlenk, A. Wagner, F.-P. Weiss, Annals of Nuclear Energy 34, 36 (2007)

Project partner

· Physikalisch-Technische Bundesanstalt (PTB) Braunschweig, Germany

Counter-current flow limitation experiments
at the TOPFLOW test facility

Christophe Vallée, Matthias Beyer,
Dirk Lucas, Horst-Michael Prasser[1]

In the event of a loss-of-coolant-accident (LOCA) in a pressurized water reactor, emergency strategies have to be mapped out in order to guarantee the reliable removal of the decay heat from the reactor core. During a hypothetical small break LOCA with failure of the high pressure emergency core cooling system, the decay heat has to be released to the secondary circuit over the steam generators, via a two-phase natural circulation in the primary circuit. If the water level in the reactor pressure vessel falls below the hot leg inlet, steam only flows to the steam generator. In this case, the natural circulation breaks down and switches to the reflux condenser mode, which means that the steam coming from the reactor pressure vessel condenses in the vertical U-tubes of the steam generator. As it flows down the tubes, part of the condensate has to stream back over the hot leg to the upper plenum in counter-current to the steam flow.

The horizontal stratified counter-current flow of condensate and steam is only stable for a certain range of flow rates. In case of high steam flow rates, part of the condensate can be clogged in the hot leg marking the beginning of the counter-current flow limitation (CCFL): the hot leg and steam generator are flooded, which decreases the water level in the reactor pressure vessel and reduces the core cooling. The simulation of CCFL conditions, which are dominated by 3D effects, requires the use of a computational fluid dynamics (CFD) approach. These methods are not yet mature and have to be validated by sound experiments before they can be applied to nuclear reactor safety analyses. Therefore, dedicated experimental data are needed with high resolution in space and time, ideally at reactor typical conditions. For these purposes, a model of the hot leg of a pressurized water reactor was built at the TOPFLOW test facility of the FZD.

The hot leg model
The hot leg model (Figs. 1 and 2) is devoted to optical measurement techniques, so a flat test-section design was chosen
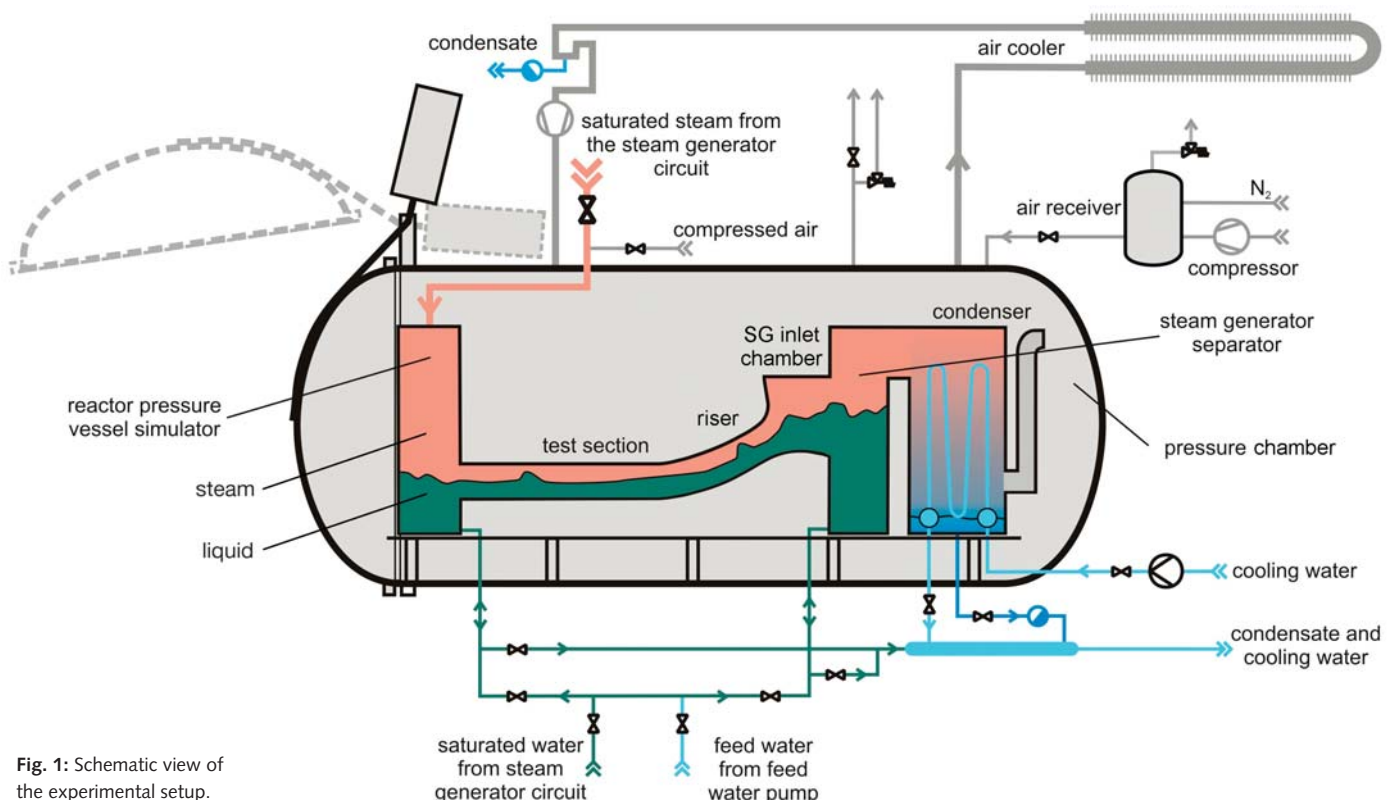

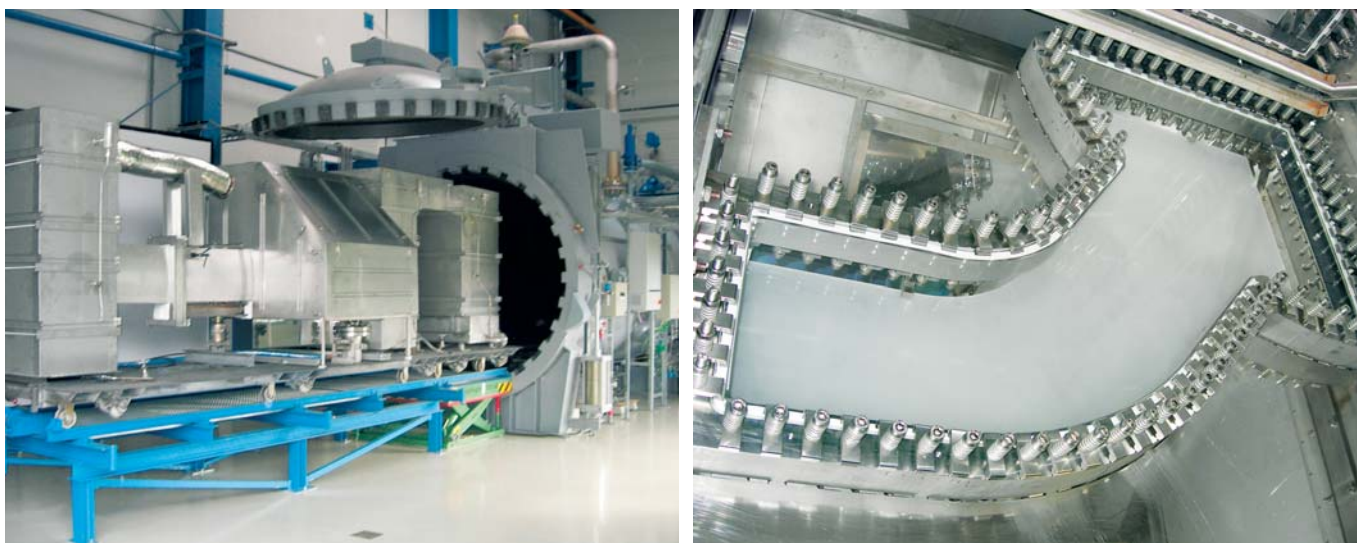**Fig. 1:** Schematic view of the experimental setup.

Fig. 2: The test section in front of the pressure chamber (left) and the transparent part of the hot leg model (right).

with a width of 50 mm. The test section represents the hot leg of the German *Konvoi* pressurized water reactor at a height scale of 1:3, which corresponds to a channel height of 250 mm in the straight part of the hot leg. The test-section is mounted between two separators, one simulating the reactor pressure vessel and the other being connected to the steam generator inlet chamber. This allows performing co-current as well as counter-current flow experiments. The hot leg model is operated in the pressure chamber of the TOPFLOW facility (Fig. 1), which is used for high-pressure experiments under pressure equilibrium with the inside atmosphere of the chamber. This new operation method was developed at the FZD and enables the application of optical observation techniques at reactor typical

conditions (i.e. pressures up to 5 MPa and temperatures up to 264°C). The presented experiments focus on the flow structure observed in the region of the riser and of the steam generator inlet chamber (Fig. 2, right) during counter-current flow. They were carried out in the frame of a current research project funded by the German Federal Ministry of Economics and Technology.

As an example, one of the experiments performed at a system pressure of 5.0 MPa and a temperature of 262°C may serve to explain the phenomena. During this experiment, a constant water flow rate of 0.72 kg/s was injected into the steam generator separator while the gas flow rate injected into the reactor pressure vessel simulator was gradually increased to reach

counter-current flow limitation conditions. The measurement of global parameters (e.g. flow rates, water levels, pressures) was complemented by high-speed video observations for local information on the flow structure (Fig. 3). Thanks to the rectangular cross-section geometry, the pictures of the flow deliver a detailed view of the stratified interface as well as of the distribution of dispersed structures (droplets and bubbles). This kind of visualization of steam/water flows over large windows at reactor typical conditions is a world first.

At the beginning of the experiment, the counter-current flow is stable (Fig. 3-a): a thin supercritical water layer (i.e. Froude number > 1) flows down the riser to the reactor pressure vessel simulator. Just small waves are observed, which do not affect

(a) stable counter-current flow
t   = 60.00 s
$\dot{m}_G$ = 0.81 kg/s
$\dot{m}_{L,d}$ = 0.71 kg/s

(b) during counter-current flow limitation
t   = 80.25 s
$\dot{m}_G$ = 0.92 kg/s
$\dot{m}_{L,d}$ = 0.23 kg/s

(c) during counter-current flow limitation
t   = 125.28 s
$\dot{m}_G$ = 0.99 kg/s
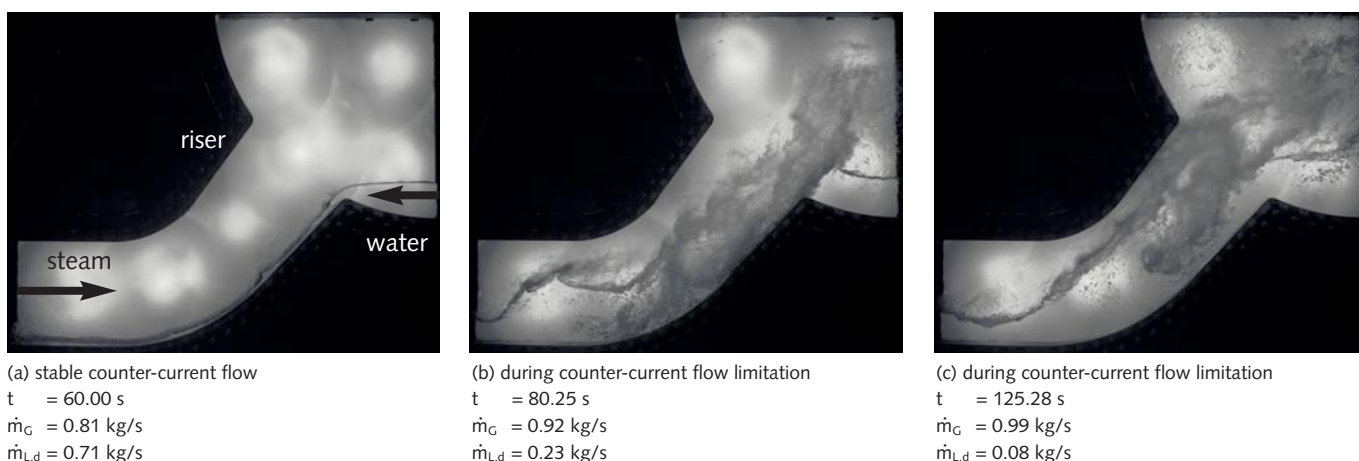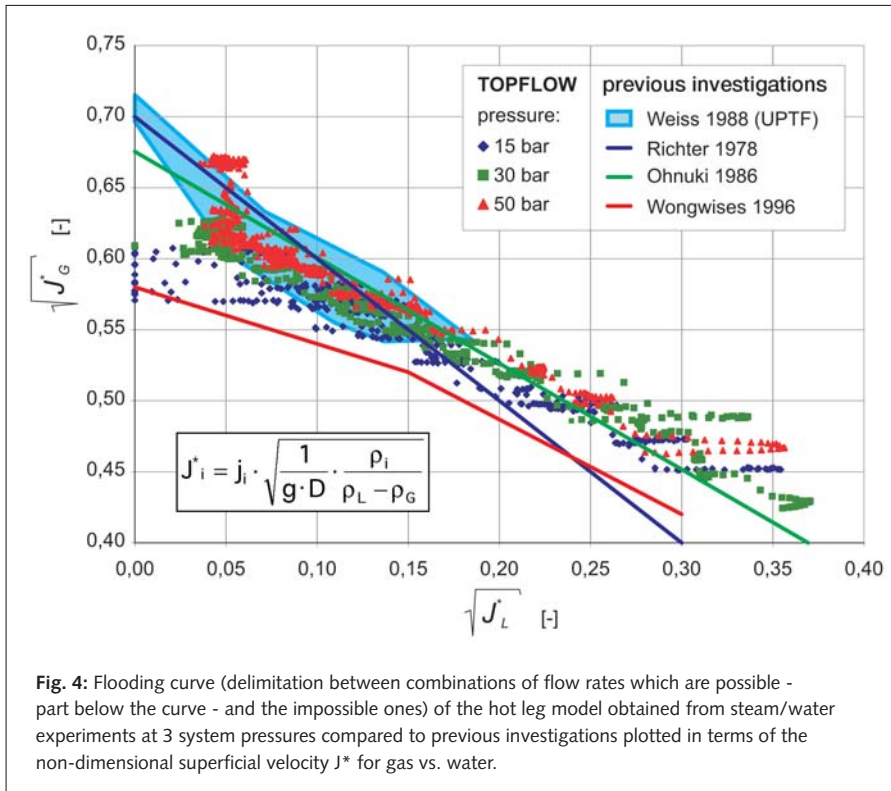$\dot{m}_{L,d}$ = 0.08 kg/s

Fig. 3: Evolution of the flow during a steam/water counter-current flow limitation experiment performed at 5.0 MPa and 262°C with $\dot{m}_L$ = 0.72 kg/s.

$$J^*_i = j_i \cdot \sqrt{\frac{1}{g \cdot D} \cdot \frac{\rho_i}{\rho_L - \rho_G}}$$

Fig. 4: Flooding curve (delimitation between combinations of flow rates which are possible - part below the curve - and the impossible ones) of the hot leg model obtained from steam/water experiments at 3 system pressures compared to previous investigations plotted in terms of the non-dimensional superficial velocity J* for gas vs. water.

References

[1] *Experimental study on the air/water counter-current flow limitation in a model of the hot leg of a pressurized water reactor*, Deendarlianto, C. Vallée, D. Lucas, M. Beyer, H. Pietruske, H. Carl, Nuclear Engineering and Design 238/12 (2008), 3389 – 3402

[2] *Air/water counter-current flow experiments in a model of the hot-leg of a pressurized water reactor*, C. Vallée, Deendarlianto, M. Beyer, D. Lucas, H. Carl, Journal of Engineering for Gas Turbines and Power - Transactions of the ASME 131/2, 022905 (2009)

[3] *Experimental investigation and CFD simulation of horizontal stratified two-phase flow phenomena*, C. Vallée, T. Höhne, H.-M. Prasser[1], T. Sühnel, Nuclear Engineering and Design 238/3 (2008), 637 – 646

Project partners

· ETH Zürich, Switzerland[1]
· Gadjah Mada University, Yogyakarta, Indonesia
· Université Catholique de Louvain, Belgium

the flow. After an increase of the steam flow rate from 0.81 to 0.92 kg/s, water accumulates in the horizontal part of the channel due to a flow reversal at the interface. The high gas velocity generates waves and slugs at the water surface (Fig. 3-b): bubbles are entrained in the liquid phase and the interface is torn into droplets, especially at wave crests. The slugs collapse in the riser but droplets detach at the slug front, transporting water to the steam generator inlet chamber. At the junction between horizontal channel and riser, a recirculation zone is observed: the water flowing down the riser from the steam generator inlet chamber is deflected by the slugs arriving from the other direction. The discharge water flow through the test-section ($\dot{m}_{L,d}$) can be obtained from the water level increase in the reactor pressure

vessel simulator. At this stage, it has been reduced to 0.23 kg/s. With a further increase of the steam flow rate to 0.99 kg/s, the discharge water flow is reduced to 0.08 kg/s. As a consequence, the flow shows highly mixed two-phase zones (Fig. 3-c). Big slugs are observed which flow up the riser and transport water into the steam generator separator, where the water accumulates.

Results of counter-current flow limitation are usually presented in a flooding diagram by plotting the dimensionless superficial velocity J* of the air versus that of the discharge water, which is measured from the water level increase in the reactor pressure vessel simulator. The flooding curve (Fig. 4) indicates the maximum water flow rate for a given gas flow rate and

therefore delimits the possible combinations of flow rates from the impossible ones. Fig. 4 compares the data obtained from the experiments in the hot leg model with different results obtained for similar geometries (i.e. a horizontal conduit connected to a riser) available in the literature: Richter et al. (1978), Ohnuki et al. (1986), Weiss et al. (1988) and Wongwises (1996). The overall agreement with previous investigations performed in pipes shows that the rectangular cross-section of the hot leg model does not influence counter-current flow limitation. In the near future, image processing methods will be applied in order to extract local quantitative information from the high-speed camera images. This will be used for comparison with computational fluid dynamics simulations.

Ultra high speed electron beam X-ray tomography
for two-phase flows

Uwe Hampel, Frank Fischer

Multiphase flows occur in many industrial areas, such as in nuclear light water reactors, chemical reactors, hydrodynamic machines, oil exploration, biochemical processing and water management. A key issue to understand the physical principles governing such flows is the availability of adequate measurement techniques which enable to measure and visualize multiphase flows at very high speed and with high spatial resolution. A good candidate technology is X-ray computed tomography (CT). However, standard computed tomography scanners as used in medicine are much too slow since they employ mechanically moving parts for scanning.

For industrially relevant multiphase flows, velocities in the range of 1 m/s and higher are common. Therefore, a tomography technique is required which can scan the flow at rates of 1000 frames per second and even higher. This can be achieved by electron beam tomography, which offers both high spatial and temporal resolution along with non-intrusiveness and good linearity in density resolution.

In order to use this technology for flow measurement, we developed a dedicated electron beam CT scanner which was optimized for very fast image generation up to 7 kHz frame rate. The functional principle of the scanner is displayed in Fig. 1. Within the scanner an electron beam of 150 keV maximum energy is generated by means of an electron gun. The beam first passes an electron lens system, which provides beam centering and focusing, and then an electromagnetic deflection system, which allows rapid beam deflection in two directions. On the farther end of the scanner resides a

semicircular target made of a tungsten alloy which stops the electrons, thereby producing X-rays within a small focal spot (see Fig. 4). By fast scanning of the beam across the target using the beam deflection unit, a moving focal X-ray spot is produced which rapidly circulates around the target. This electron beam system replaces the rotating X-ray tube of standard medical CT scanners and enables scanning frequencies well above 1 kHz.

For measuring the X-ray attenuation caused by an object residing in the centre of the target, a circular X-ray detector is arranged at the inner side of the opening in the scanner head. This detector comprises 240 fast semiconductor pixels

which can be sampled at a rate of up to 1 MHz by dedicated detector electronics. Additional components include a high voltage supply, vacuum system, beam monitoring system and control PC. The developed scanner, which is named ROFEX (ROssendorf Fast Electron beam X-ray scanner), can be operated at beam powers of up to 10 kW at scanning rates of up to 7,000 frames per second. The spatial resolution is about 1 mm and objects of up to 100 mm diameter can be investigated. A limiting factor is the maximum X-ray energy of 150 keV, which prohibits the penetration of steel or other dense materials. Fig. 2 shows the scanner mounted at a vertical test section of the TOPFLOW facility. Here, the test section is a 50 mm
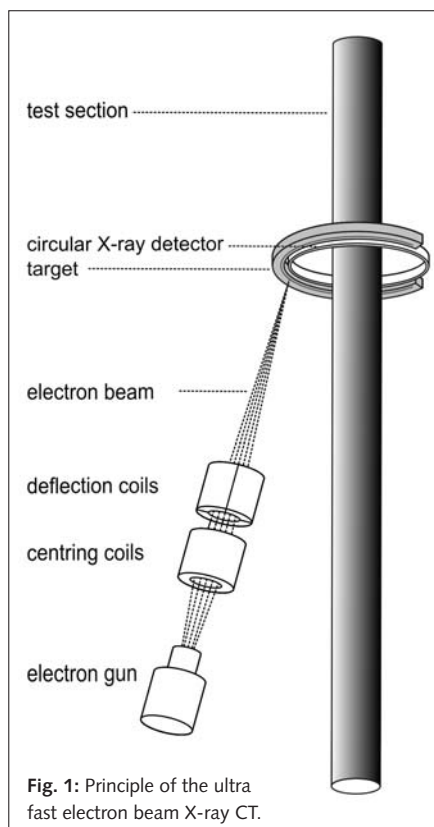

Fig. 1: Principle of the ultra fast electron beam X-ray CT.

Fig. 2: ROFEX scanner at a vertical test section of the TOPFLOW facility.

pipe made of a titanium alloy with 1.5 mm wall thickness, which will be used to study steam-water two-phase flows under pressures of up to 7 MPa and a corresponding saturation temperature of 284 °C.

As an example, Fig. 3 shows X-ray tomography images taken with the ROFEX scanner from a bubble column. Such devices are frequently used in chemical industry where gases and liquids are brought into contact for reaction. Efficient reaction is ensured when gas is finely dispersed into the liquid while slug flow regimes are to be avoided because of low interfacial area density and pulsating mass transfer. In such devices, the flow patterns and their transitions follow complex evolutions which are not yet fully understood. In the given example, the ROFEX scanner acquired cross-sectional images of the 60 mm column with a rate of 1 kHz. For the first time, this enables a complete visualization of the gas-liquid structure including the phase boundary, which is necessary to measure further process parameters, such as the local gas hold-up and interfacial area density.
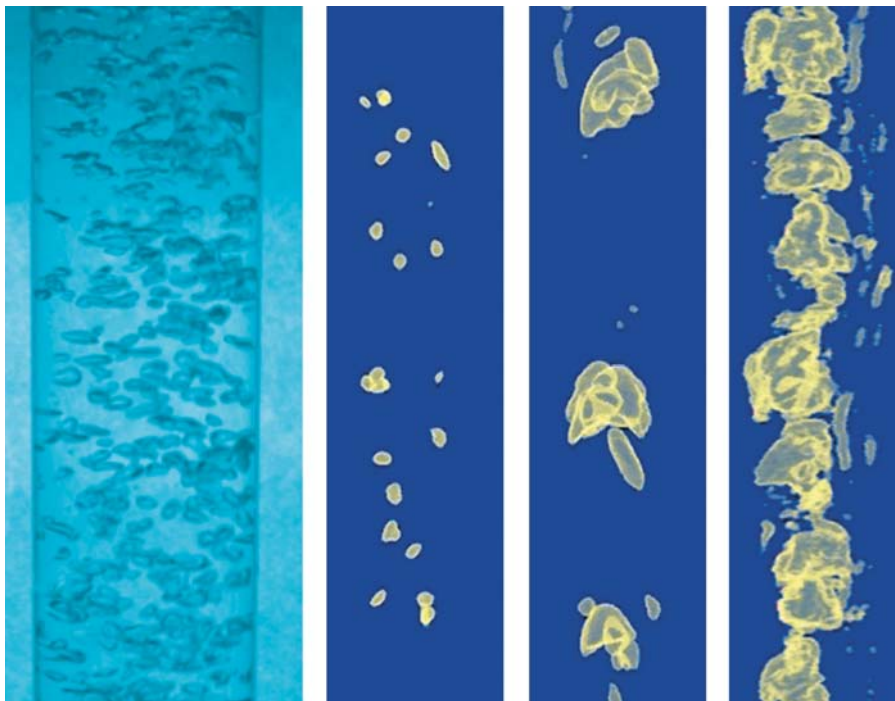
With the development and commissioning of an ultra fast electron beam X-ray CT scanner, for the first time world wide, we are able to image complex and highly dynamic multiphase flows in unprecedented spatial and temporal detail. In this way only, it will be possible to understand and perhaps model the complex physics of multiphase flows. This will greatly enhance our ability to optimize technical processes involving such flows and to assess safety issues associated with the operation of nuclear and chemical installations.

Fig. 3: Optical image (left) and three-dimensional ROFEX images (right) of the gas distribution in a bubble column.

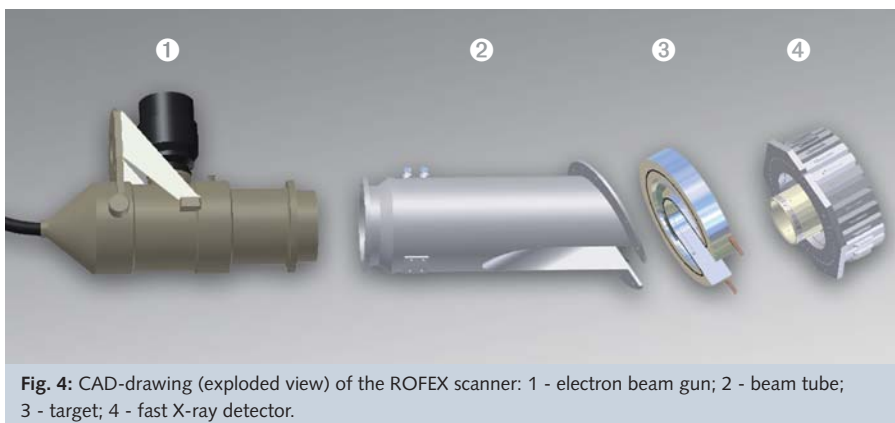**Fig. 4:** CAD-drawing (exploded view) of the ROFEX scanner: 1 - electron beam gun; 2 - beam tube; 3 - target; 4 - fast X-ray detector.

References

[1] *Ultra fast limited-angle type X-ray tomography*, M. Bieberle, F. Fischer, E. Schleicher, D. Koch, K. S. D. C. Aktay, H.-J. Menz, H.-G.Mayer, U. Hampel, Applied Physics Letters 91, 123516 (2007)

[2] *Simulation study on electron beam X-ray CT arrangements for two-phase flow measurements*, M. Bieberle, E. Schleicher, U. Hampel, Measurement Science and Technology 19, 094003 (2008)

[3] *An ultra fast electron beam X-ray tomography scanner*, F. Fischer, D. Hoppe, E. Schleicher, G. Mattausch, H. Flaske, R. Bartel, U. Hampel, Measurement Science and Technology 19, 094002 (2008)

Project partners

· Institut für Kernenergetik und Energiesysteme, Universität Stuttgart, Germany
· Fraunhofer-Institut für Elektronenstrahl- und Plasmatechnik Dresden, Germany

Advanced measuring techniques
for liquid metal flows in fast neutron nuclear reactors

Sven Eckert, Dominique Buchenau,
Gunter Gerbeth

Design and optimization of the thermal hydraulics of liquid metal cooled nuclear reactors are based on numerical simulations of the heat and mass transfer processes of the related flow field. However, velocity measurements in opaque liquid metal flows still represent a challenging task as commercial measuring systems are not available for such melts. During the last 10 years, considerable effort has been spent at the FZD on the development and qualification of techniques to measure the

velocity in liquid metal flows. Significant progress has been achieved especially in the field of non-invasive measuring techniques, with new developments concerning electromagnetic flow meters and the Ultrasound Doppler method, respectively.

A multitude of different electromagnetic flow-meter designs are known, the majority of which, however, need an electrical contact to the liquid metal in order to measure the electric potential difference. The working conditions relevant to nuclear systems, such as high

temperatures, interfacial effects or corrosion, prohibit this approach. A liquid metal flow inside an external magnetic field gives rise to electrical currents in the melt which cause a deformation of the applied magnetic field. Such a deformation can be measured outside the fluid volume, and this information can be used to reconstruct the velocity field. Based on this principle, new types of inductive flow meters were developed at the FZD, which operate in a fully contactless manner. A schematic view of the new flow meter is shown in Fig. 1. Operation is based on the detection of the asymmetry of the magnetic field caused by the flow. Besides the voltage difference between the two receiver coils, the device also provides two additional quantities: phase and frequency. Such additional information significantly improves the reliability of the measured flow rate [1]. The feasibility and the robustness of our approach were successfully demonstrated at various liquid metal loops of temperatures up to 550 °C, e.g. at the lead-bismuth (PbBi) loop of the Belgian Nuclear Research Centre SCK•CEN in the framework of the European project EUROTRANS ("European research program for the transmutation of high-level nuclear waste in an accelerator driven system").

Because of its ability to work in opaque fluids and to deliver complete velocity profiles in real time, the Ultrasound Doppler Velocimetry (UDV) technique has become very attractive for liquid metal applications. Measurements can be done through the channel wall as well as in direct contact with the liquid metal. Many applications in the nuclear field are related to liquid metal two-phase flows. For such kinds of flows, it was successfully shown that the UDV technique can simultan-
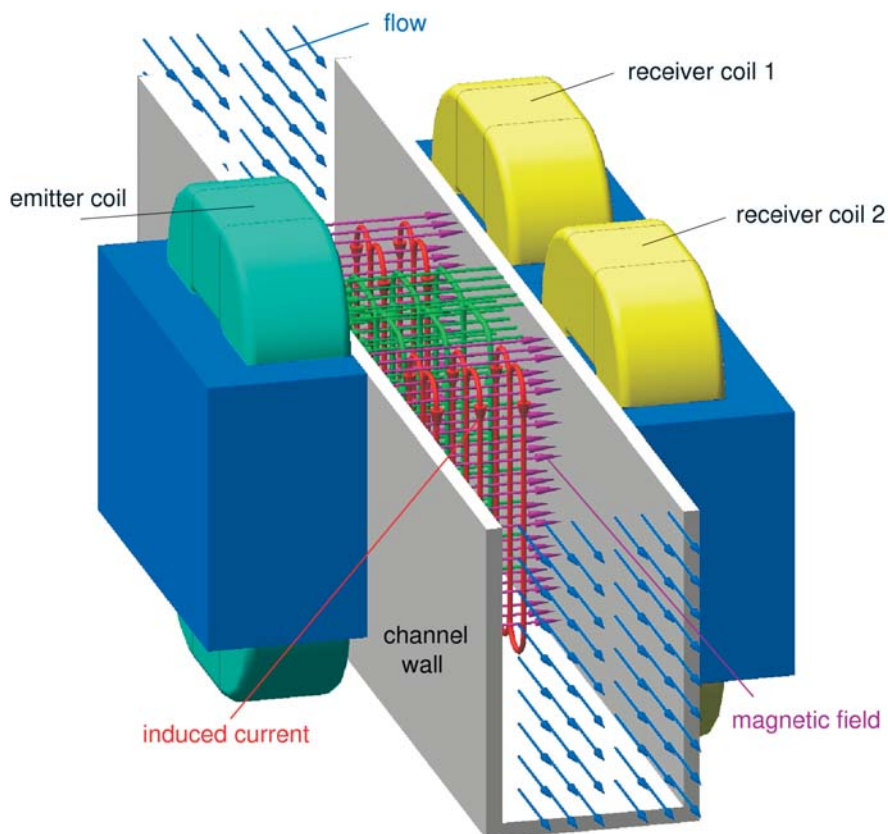

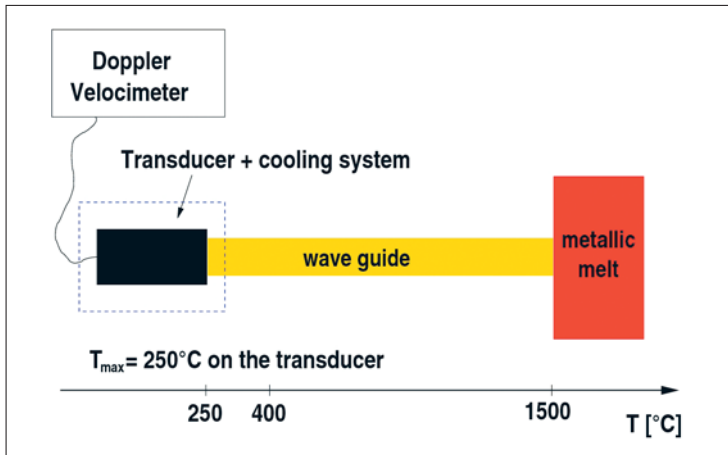**Fig. 1:** Schematic view of the electromagnetic flow meter.

Fig. 2: Concept of an ultrasonic sensor with integrated acoustic waveguide: schematic view (left) and picture of a sensor for melt temperatures up to 750°C (right).

eously deliver both the bubble and the liquid velocity [2]. In the case of hot metallic melts the user is confronted with a number of specific problems: first of all, the application of conventional piezo-electric transducers is usually restricted to maximum temperatures below 200 °C. Moreover, the transmission of a sufficient amount of ultrasonic energy from the transducer into the fluid has to be guaranteed. Therefore, the acoustic coupling and the wetting conditions are important issues. A new concept of an ultrasonic transducer with integrated acoustic wave guide was designed [3] in order to achieve a thermal and chemical decoupling between the transducer and the hot liquid metal. Stainless steel was selected as wave-guide material. The ultrasonic sensor consisting of the piezo-electric element and the acoustic wave guide is shown in Fig. 2. The wave guide is fabricated from a stainless steel foil with a thickness of 0.1 mm, which is wrapped axially around a capillary tube. It is closed at the front end by means of laser beam welding. This surface is in direct contact

with the melt and has to be prepared before the measurements to obtain a sufficient wetting with the liquid metal. Typically, the wave guides have an outer diameter of about 8 mm and a length between 200 and 1000 mm. The operability of such wave guides has been demonstrated in PbBi at 300 °C as well as in liquid aluminum and CuSn alloys at temperatures up to 750 °C.

With both measuring techniques, contact-less flow-rate sensor and Ultrasound Doppler Velocimetry, we contribute to the European projects EUROTRANS and VELLA ("Virtual European lead laboratory"). They are related to the development of a PbBi based target for nuclear spallation sources in transmutation systems, where transuranium elements are irradiated with fast neutrons in order to reduce the proportion of long-lived isotopes enclosed in nuclear waste. Liquid metal measuring techniques are also part of the upcoming European project CP-ESFR in the field of liquid sodium cooled fast reactors. Moreover, there are many

industrial applications requiring velocity measurements in molten metals ranging from molten tin in float-glass production to liquid steel casting, where such techniques could successfully be applied.

References

[1] *Verfahren und Anordnung zur kontaktlosen Messung des Durchflusses elektrisch leitfähiger Medien*, J. Priede, G. Gerbeth, D. Buchenau, S. Eckert, Patent DE 10 2006 018 623 B4 (2008)

[2] *The flow structure of a bubble-driven liquid metal jet in a horizontal magnetic field,* C. Zhang, S. Eckert, G. Gerbeth, Journal of Fluid Mechanics 575 (2007), 57 – 82

[3] *Velocity measurement techniques for liquid metal flows*, S. Eckert, A. Cramer, G. Gerbeth, in "Magnetohydrodynamics – Historical Evolution and Trends", S. Molokov, R. Moreau, H.K. Moffatt (eds.), Springer-Verlag (2007), 275 – 294

Collaboration

· DFG Collaborative Research Center SFB 609, Technische Universität Dresden, Germany

Flux dependence of defect cluster formation
in neutron irradiated weld material

© R. Weisflog

Frank Bergner, Uwe Birkenheuer,
Andreas Ulbricht

The core-belt region of the reactor pressure vessel (RPV) of a nuclear power plant (NPP) is exposed to intense neutron irradiation, and the fast neutrons cause degradation of the mechanical properties. In order to guarantee the structural integrity of the RPV throughout its operational lifetime, surveillance programs are implemented prior to initial commissioning of a nuclear power plant. According to these programs specimens of the RPV steel are inserted into capsules and placed in special surveillance channels. At these positions, the fast neutron flux (number of neutrons per unit area and unit time) exceeds the flux at the RPV wall by a "leading factor" (typically between 1.5 and 12). The specimens are taken from the surveillance capsules at regular intervals in order to undergo mechanical tests in hot cell labs (Fig. 1). The mechanical properties are then assumed to be characteristic of

the RPV material at an instant of time corresponding to the irradiation time of the specimen multiplied by the leading factor. However, this procedure is only applicable if flux effects are either completely absent, i.e. degradation depends on fluence only, or result in a conservative prediction of the behavior of the RPV material. At this point, the basic interest in the dependence of the mechanical properties and the underlying microstructure on neutron flux becomes evident.

How to separate flux effects on the microstructure

The primary irradiation parameter governing the degradation of material properties is neutron fluence, Φ, i.e. neutron flux, φ, multiplied by exposure time, t. Neutron flux is a secondary parameter, though of primary technical importance. In order to separate flux effects from the dominant dependence on fluence, it is necessary to vary the value of flux while keeping the value of fluence

constant. An appropriate pair of samples was selected from German irradiation programs. Identical samples of weld material containing 0.22 wt% Cu were exposed to fluxes, $\varphi_1 = 0.06 \times 10^{12}\,\mathrm{cm^{-2}s^{-1}}$ and $\varphi_2 = 2.08 \times 10^{12}\,\mathrm{cm^{-2}s^{-1}}$ (E > 1 MeV), differing by a factor of 35. The neutron fluence, $\Phi = \varphi\,t = 2.2 \times 10^{19}\,\mathrm{cm^{-2}}$, was made to agree for both conditions by choosing irradiation times, $t_1 = 11.6$ years vs. $t_2 = 122$ days.
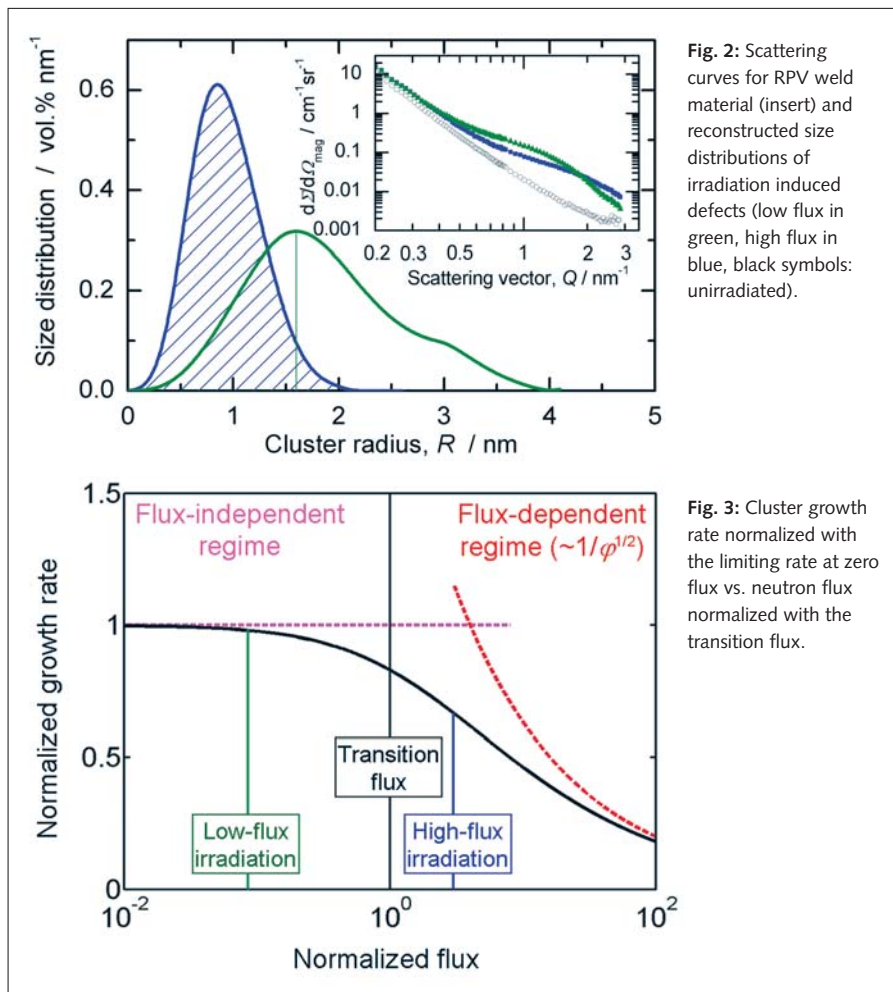
Samples of these material conditions were analyzed by means of small-angle neutron scattering (SANS) at the beamline V4 of the Helmholtz Centre Berlin for Materials and Energy. The results are presented in Fig. 2 in terms of scattering curves, i.e. measured scattering cross section vs. scattering vector, Q (see insert), and in terms of reconstructed size distributions of the irradiation induced defects [1]. We have observed that (1) the total volume fraction of irradiation induced defect-solute clusters (hatched area for blue curve) agrees for both values of neutron flux and assumes a value of 0.52 vol.%, and (2) the peak radius of the size distribution (marked for the green curve) is increased for low-flux irradiation by the factor 2 (0.85 nm vs. 1.6 nm). Mechanical impact testing of the same material did not reveal any significant dependence of the brittle-to-ductile transition temperature shift, ΔT_{41}, on flux (119 K vs. 111 K). It is important to note that the latter result is consistent with state-of-the-art surveillance procedures. From the viewpoint of physical understanding we have to answer two questions: Why does the cluster size exhibit a pronounced flux dependence, and why, in spite of that, is there no difference in the shift of the transition temperature?

Simulating cluster growth by means of reaction rate theory

The constituents of our rate theory model are the balance equations for point defects (vacancies and self-interstitial atoms) and for Cu-clusters. We assume the ratio of irradiation enhanced and thermal Cu-diffusivity to be given by the ratio of steady-state and equilibrium concentration of vacancies. Based on asymptotic considerations of the equations involved in the model, we have found that there are two different flux regimes (Fig. 3). In the low-flux regime, the growth rate of Cu-rich clusters is independent of flux. In this case, the dominant process causing the loss of vacancies is the disappearance at sinks like grain boundaries or dislocations. The high-

flux regime with vacancy-interstitial recombination as prevailing mechanism of vacancy loss is characterized by an inverse proportionality of the growth rate with the square root of flux. The rate theory model also yields an expression for the transition flux estimated to be $0.7 \times 10^{12} \, cm^{-2}s^{-1}$ under the present conditions. In other words, the investigated low-flux irradiation of the weld material belongs to the flux-independent regime whereas for high-flux irradiation a reduced rate of cluster growth is expected in qualitative agreement with the experimental observation. Existing disagreement on the magnitude of the flux effect is attributed to the effect of the alloying elements not yet taken into account in the model.

In order to bridge the gap between nanoscale features and macroscopic mechanical properties, it is important to note that state-of-the-art models generally predict the material's resistance to plastic deformation (strength) to depend on both volume fraction and size of irradiation induced defect-solute clusters. Increase of strength is in turn correlated with the transition temperature shift. Thus, our experimental findings rule out any model that predicts a pronounced size dependence. The results substantiate the hypothesis that the mechanical properties are mainly determined by the total volume fraction of the clusters whereas cluster size seems to be of minor influence [2]. However, this hypothesis has to be confirmed by further studies.

Fig. 2: Scattering curves for RPV weld material (insert) and reconstructed size distributions of irradiation induced defects (low flux in green, high flux in blue, black symbols: unirradiated).

Fig. 3: Cluster growth rate normalized with the limiting rate at zero flux vs. neutron flux normalized with the transition flux.

References

[1] *Flux dependence of cluster formation in neutron-irradiated weld material*, F. Bergner, A. Ulbricht, H. Hein[1], M. Kammel[2], Journal of Physics: Condensed Matter 20, 104262 (2008)

[2] *SANS response of VVER440-type weld material after neutron irradiation, post-irradiation annealing and reirradiation*, A. Ulbricht, F. Bergner, J. Böhmert, M. Valo[3], M.-H. Mathon[4], A. Heinemann[2], Philosophical Magazine 87, 1855 (2007)

Project partners
· AREVA NP GmbH, Erlangen, Germany[1]
· Helmholtz Centre Berlin for Materials and Energy, BENSC, Germany[2]
· VTT Technical Research Centre of Finland, Espoo, Finland[3]
· Commissariat à l'Energie Atomique, Centre de Saclay, France[4]
· Centro de Investigaciones Energéticas Medioambientales y Tecnológicas, Madrid, Spain
· Electricitè de France, Site des Renardieres, France
· Gesellschaft für Reaktorsicherheit, Köln, Germany
· Kurchatov Institute, Moscow, Russia
· Studiecentrum voor Kernenergie•Centre d'Etude de l'énergie Nucléaire, Mol, Belgium

Analytical neutron transport solution
for a pulsed subcritical transmutation system

Bruno Merk, Frank-Peter Weiss

The underground storage in deep geological repositories has been accepted worldwide as the strategy for the final disposal of radioactive waste. Partitioning and Transmutation (P&T) is an appropriate means to reduce the share of extremely long-lived radionuclides, which also helps to relieve safety requirements at the disposal site and to reduce the necessary isolation time. The development of the accelerator driven system (ADS) technology for the transmutation of mainly plutonium and minor actinides is vigorously pursued in the EURATOM framework program. ADSs are dedicated burners of long-lived radionuclides.

ADSs connect a proton accelerator with a subcritical reactor core (see Fig. 1). By spallation reactions in a heavy metal target, the accelerated protons generate neutrons in the center of the system. These external source neutrons maintain the chain reaction, thus enabling continuous power production at a quasi-stationary level in the subcritical core. The neutron flux in the core decays rapidly as soon as the external neutron source is switched off. The neutron physical behavior of ADSs is currently under investigation in the European Integrated Project EUROTRANS of the 6th EU Framework Program. Kinetic neutron physics experiments for ADS technology are performed in the ECATS domain of this project at the YALINA Booster facility in Minsk, Belarus, and later on at the GUINEVERE facility at the Belgian Nuclear Research Centre (SCK•CEN).

In order to optimize the design and safety of ADSs, it is important to be able to properly analyze the space-time behavior of the neutron flux in current, and planned, European experiments. Mostly, analysis of subcritical kinetic experiments is still based on methods originally developed for the analysis of experiments in critical reactors. However, the use of these methods is limited since they were derived from the zero dimensional point kinetics equations. The point kinetics in turn represents an approximated solution of the diffusion equation. Recent analyses of such kinetic experiments using these methods have shown unacceptable deviations between experiments and theoretical predictions. Detailed mathematical and physical investigations reveal that due to their limitations neither the point kinetics nor the diffusion equation can properly reproduce the kinetic system behavior of subcritical systems. In order to handle this problem, we have established a new approach solving the time dependent telegrapher's or P_1 equation. Analytic approximation solutions have been developed and applied to the pulsed neutron source problem described above. The results of these new approximation solutions are compared to the diffusion equation.
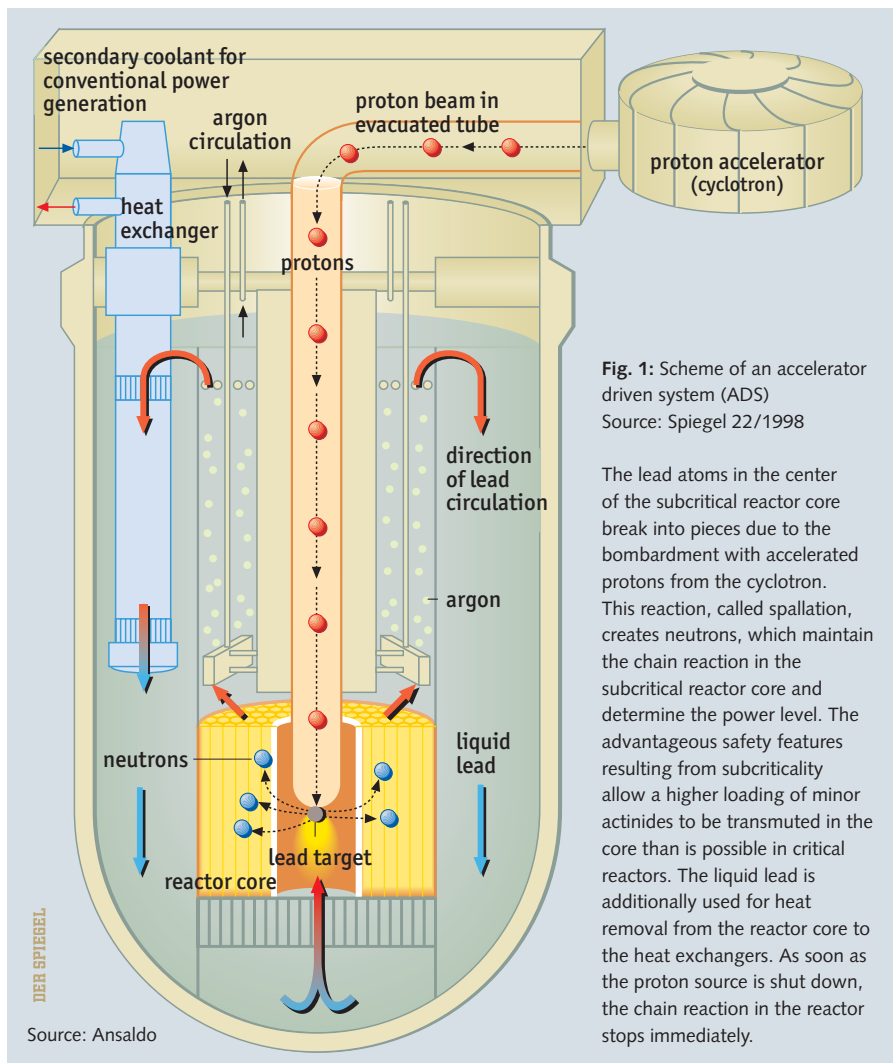

Fig. 1: Scheme of an accelerator driven system (ADS)
Source: Spiegel 22/1998

The lead atoms in the center of the subcritical reactor core break into pieces due to the bombardment with accelerated protons from the cyclotron. This reaction, called spallation, creates neutrons, which maintain the chain reaction in the subcritical reactor core and determine the power level. The advantageous safety features resulting from subcriticality allow a higher loading of minor actinides to be transmuted in the core than is possible in critical reactors. The liquid lead is additionally used for heat removal from the reactor core to the heat exchangers. As soon as the proton source is shut down, the chain reaction in the reactor stops immediately.
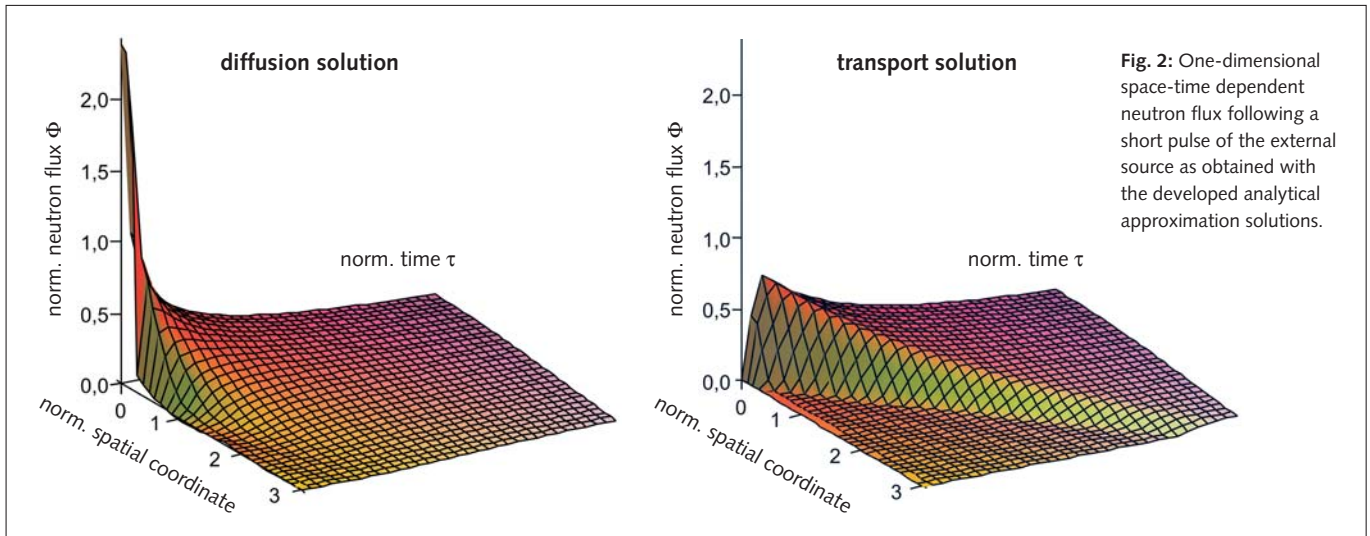
Fig. 2: One-dimensional space-time dependent neutron flux following a short pulse of the external source as obtained with the developed analytical approximation solutions.

In their textbook "The physical theory of neutron chain reactors", Weinberg and Wigner already characterized the telegrapher's equation as the correct time dependent P_1 approximation to Boltzmann's neutron transport equation. The telegrapher's equation is second order with respect to time, compared to the first order diffusion equation. Due to this property, the P_1 solution is capable of describing retardation effects, which include the occurrence of a well-defined wave front of neutron propagation and the existence of a residual disturbance persisting at all points traversed by the wave front. Contrary to this, the propagation velocity of a neutron flux perturbation is infinite in the diffusion equation. A change in the external source immediately produces a disturbance everywhere in the system. This limitation of the diffusion becomes crucial in future ADS operation. The differences can be especially observed in kinetic experiments measuring large variations of the neutron flux on very short time scales, where the influence of the propagating neutron flux wave front cannot always be ignored.

Fig. 2 provides a qualitative comparison of the results obtained with the diffusion and telegrapher's equation, the spatial coordinate pointing to the front and time evolution to the right. The neutron flux transient shown there is initiated by a neutron pulse from an external neutron source located in the center part of the homogenized system. The pulse is repre-

sented by a Dirac delta function. The homogenized system has to be derived from the real system (Fig. 1) using numerical neutron transport methods. The initial value of the neutron flux is zero in the whole system. The experiment starts when the external source pulse occurs in the center of the symmetric one-dimensional system at time zero. The neutrons spread out immediately in both the diffusion and transport solution. Nevertheless, only the solution obtained with the P_1 equation depicts a clearly defined wave front whereas in the diffusion solution the perturbation caused by the external source pulse propagates with an infinite velocity. The excessive flux peak occurring in the center, immediately after the pulse, is a side effect of this unrealistically high propagation velocity since the response to the pulse is created by multiplication in the whole system. This is an artifact caused by the diffusion approximation. In fact, the propagation of the perturbation takes some time until it reaches the outer zone of the system. The velocity of the wave propagation approximates the neutron velocity divided by $\sqrt{3}$.

Obviously, the telegrapher's or P_1 equation provides additional insight into the system behavior. Such additional information is indispensible in cases where detailed information on the short time behavior of the system is required. This applies to current ADS experimental setups, which imply strong external neutron sources as well as measurements at time scales of the

order of the prompt neutron generation time. The neutron wave travels about 20 centimeters during one neutron generation. On the one hand, measurement is therefore influenced by the pulses if the repetition rate is low. On the other hand, it is impeded by a time delay if the detectors are far away from the source. Due to the reasons mentioned above, the approximated neutron transport solutions will be used to develop new analysis methods for kinetic ADS experiments.

References

[1] *An analytical solution for a one dimensional time dependent neutron transport problem with external source*, B. Merk, Transport Theory and Statistical Physics 37: 5-7, 535 – 549 (2008)

[2] *An analytical approximation solution for a time dependent neutron transport problem with external source and delayed neutron production*, B. Merk, Nuclear Science and Engineering 161, 49 – 67 (2009)

Project partners

· Commissariat à l'Energie Atomique, France
· Centre National de la Recherche Scientifique, France
· Instituto Tecnológico e Nuclear, Portugal
· Studiecentrum voor Kernenergie•Centre d'Etude de l'énergie Nucléaire, Belgium
· Forschungszentrum Karlsruhe GmbH, Germany
· Royal Institute of Technology, Sweden
· Centro de Investigaciones Energeticas Medioambientales y Tecnologicas, Spain
· Ente per le Nuove tecnologie, l'Energia e l'Ambiente, Italy

THEREDA - Thermodynamic Reference Database for nuclear waste disposal in Germany

Vinzenz Brendler, Anke Richter,
Sven Gester

The disposal of radioactive waste including the assessment of its long-term safety is still an open question in Germany. In addition to the choice of a repository host rock (salt, granite, clay), a consistent and obligatory thermodynamic reference database is urgently needed. This allows to accurately assess potential failure scenarios and to make well-founded predictions about the long-term safety. Waste repository and remediation projects, in Germany especially, require comprehensive datasets also covering high temperatures and high salinities. However, available databases do not suffice and are limited in their use. This is partly due to high demands on data precision, which unfortunately results in the complete omission of many reactions having larger uncertainties. Other databases rely on heterogeneous and therefore inconsistent data leading to incorrect model calculations [1].

A new reference database called THEREDA aims at overcoming these deficiencies by providing consistent thermodynamic datasets and enhancing the transparency and reliability of safety analyses. THEREDA is a joint project by the FZD and other leading institutions in the field of safety research for nuclear waste disposal in Germany and Switzerland (see list of partners). The project is jointly funded by the German Federal Ministries of Education and Research (BMBF), Economics and Technology (BMWi), and Environment, Nature Conservation and Nuclear Safety (BMU).

Fig. 1 depicts the various tasks to be addressed within this project, and also lists the different elements for which thermodynamic data (free standard enthalpy of formation (ΔG^0_f), standard enthalpy of formation (ΔH^0_f), standard entropy (S^0), standard heat capacity (C^0_p), partial molar volumina (V^0), equilibration constants (log K), and activity coefficients for species dissolved in brines and for solid solutions) have to be collected, evaluated and stored. Both data management and technical realization are integrated into a WWW-based content management system, which also provides a corresponding interactive graphical user interface (go to "http://www.thereda.de" for the current state of the project). The internal relationships, data flow and user interactions are illustrated in Fig. 2. One of the major goals of the project is to rely on open source software in order to minimize the risks of vendor dependence and incompatibilities, and to keep the long-term running costs for database maintenance low. Thus, major software components are PostgreSQL (database) and Apache (web server). For the same reason all data are stored in a generic and openly documented ASCII format.

Each dataset is documented in detail and is allocated a degree of quality. Information about solid phase modification (like "crystalline" or "amorphous") is mandatory and specific marks are designated to indicate
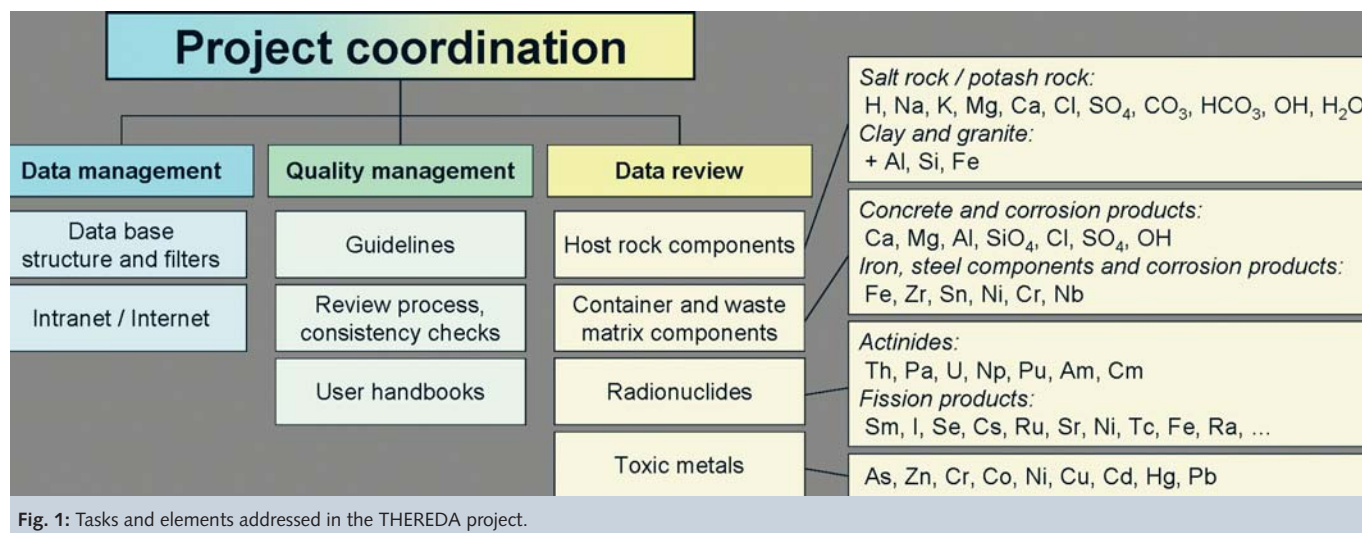

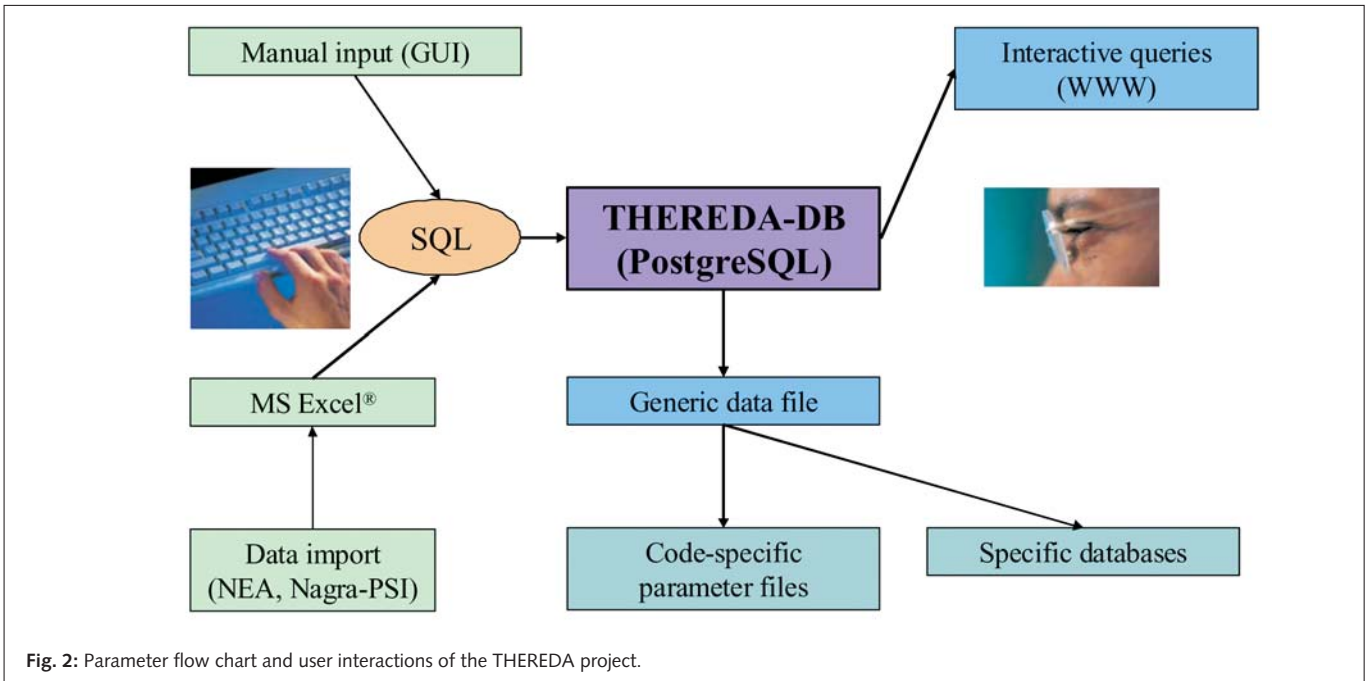**Fig. 1:** Tasks and elements addressed in the THEREDA project.

Fig. 2: Parameter flow chart and user interactions of the THEREDA project.

Final repository for nuclear waste
(Source: Bundesamt für Strahlenschutz).

whether dissolution / precipitation are kinetically controlled or not. Higher grades of quality are assigned to thermodynamic parameters derived from experimental data, namely from non-thermochemical experiments, whereas estimated values determined from Linear Free Energy Relationships and other regressions or correlations, or from studies of chemical analogs, get lower ratings. The fundamental philosophy here is that omission of species and related reactions almost always generates larger errors than using corresponding data which admit a large uncertainty. The inherent storage of all associated data uncertainties will allow for numerical uncertainty and sensitivity analyses at a later point. Furthermore, the quality of the data sources (primary or secondary literature, peer-reviewed or non-certified) is categorized.

In order to guarantee the consistency of datasets within the thermodynamic database, internal conversion paths have to be strictly followed. Other important consistency rules require linking those parameters which were originally derived simultaneously from the same experimental raw data. In addition, some parameters are linked to specific sets of chemical species and are only valid within this combination.

A special feature is that custom-designed data can be extracted from the database and converted to file formats required specifically by geochemical codes (such as EQ3/6, PHREEQC, GWB, ChemApp). This allows a widespread use for storage of radioactive waste or chemo-toxic substances and remediation of contaminated sites. Respective long-term safety analyses will be made more reliable, comparable and traceable. Moreover, we anticipate that THEREDA can serve as an instrument for research control. Priorities for future experimental programs can be given based on identifying and ranking gaps within the thermodynamic datasets.

Reference

[1] *Quality assurance in thermodynamic databases for performance assessment studies in waste disposal*, W. Voigt, V. Brendler, K. Marsh, R. Rarey, H. Wanner, M. Gaune-Escard, P. Cloke, T. Vercouter, E. Bastrakov, S. Hagemann, Pure and Applied Chemistry 79, 883 (2007)

Project partners

· Forschungszentrum Karlsruhe, Germany
· Gesellschaft für Anlagen- und Reaktor-
  sicherheit Braunschweig, Germany
· TU Bergakademie Freiberg, Germany
· AF-Colenco, Switzerland

Colloidal carbon nanotubes
and their influence on dissolved uranium

Harald Zänker

Environmental scientists and geochemists increasingly require systematic research on the risks of nanotechnology for man and the environment. They assume that fears over possible dangers of some nanotechnologies may be exaggerated, but not necessarily unfounded (cf. [1]). The concern is that the possible harm, whether real or imagined, could slow down the development of nanotechnology unless reliable information is gained on what the risks are, and how to avoid them.

Nanostructured materials, in particular engineered nanoparticles, behave as colloids if released to environmental waters, thus resembling natural colloids, which are ubiquitous in natural aquatic systems and which have been investigated for decades (cf. [2]). On the other hand, artificial nanoparticles differ from their natural counterparts. Unlike natural nanoparticles, which can vary very much in their shapes and properties, engineered nanoparticles possess well-defined properties such as distinct particle size distributions, particle shapes, functionalities etc.

One type of nanostructured materials that attract much interest are carbon nanotubes (CNTs). The demand for CNTs is expected to grow rapidly over the next decade. As these materials find their way into industrial and consumer products, their unintended release into the environment during production, use and disposal cannot be precluded. Functionalization may be a key parameter controlling the impact of CNTs on human health and environment. Even if CNTs should prove to be non-toxic, it is possible that environmental pollutants bind onto CNTs and that the transport of pollutants through the environment, as well as the bioavailability of these pollutants for aquatic organisms, can be influenced by their interaction with nanoparticles.

CNTs are very hydrophobic and tend to aggregate in aqueous solution because of high Van der Waals interaction forces along the tube exterior. As a result, they do not easily disperse in water. At first sight, CNTs should therefore not be regarded as potential mobile contaminants of aquatic systems. However, the dispersibility of CNTs in water can be increased by functionalization such as surface oxidation or by addition of surfactants.

We studied the influence of surface functionalization on the colloidal stability of CNTs [3]. CNTs were treated with concentrated HNO_3/H_2SO_4 to simulate purification steps in CNT production as well as possible alteration processes after
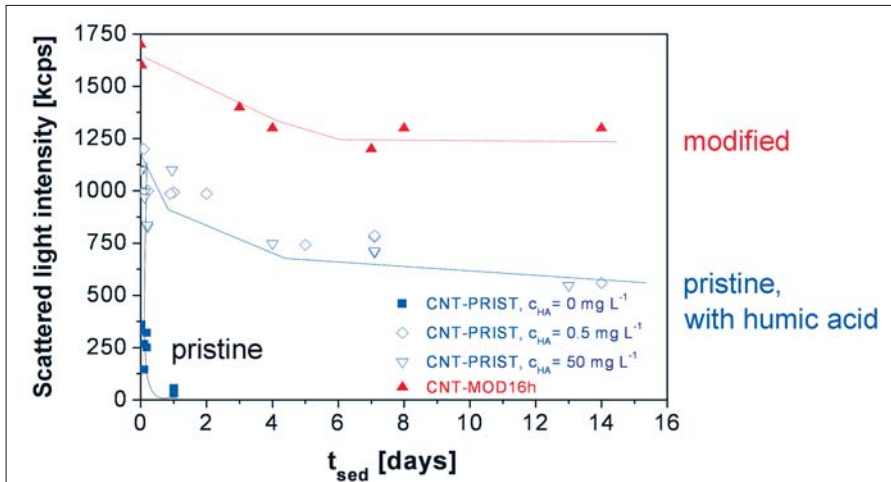
Fig. 1: Sedimentation behavior of pristine CNTs in the absence and presence of humic acid (HA) and sedimentation behavior of modified CNTs (pH 7, $c_{CNT} \leq 100$ mg L^{-1}). The suspended CNTs are indicated by the light scattered from the solution at 90° when illuminated by a laser beam.
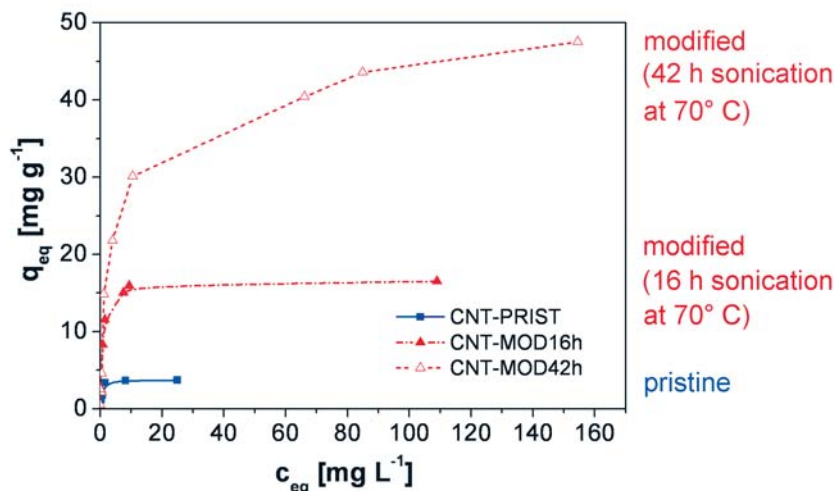

Fig. 2: Sorption isotherms of uranium(VI) on pristine and modified CNTs (pH = 5, I = 0.1 M NaClO$_4$, $p_{CO2} = 10^{-3.5}$ atm). The equilibrium surface loading by uranium, q_{eq}, depends on the uranium concentration in solution, c_{eq}, and on the intensity of the modification process (duration of sonication at increased temperature).

Finally, the sorption of heavy metal ions on CNTs was tested, and uranium was chosen as an example of a toxic heavy metal. Adsorption isotherms of hexavalent uranium on pristine and modified CNTs are depicted in Fig. 2. As can be seen, increasing amounts of uranium are adsorbed by the CNTs with an increasing degree of functionalization. A rise in U(VI) sorption capacity by more than one order of magnitude due to surface modification was observed in our experiments. The type of binding of U(VI) onto CNTs is assumed to be surface complexation between the uranyl ions and the carboxylic groups of the CNTs.

We think that transport of heavy metals such as uranium bound to CNTs through natural aquatic systems and even into biological systems such as human cells ("Trojan Horse effect") is at least conceivable. Considering the intensity of the interactions between CNTs and some environmental contaminants as well as the possibility that CNTs may act as "vehicles" for contaminants, the properties of CNTs in aquatic systems should be further investigated in order to enable prognoses of their fate, behavior and effects if released to the aquatic environment.

References

[1] *Safe handling of nanotechnology*, A.D. Maynard, Nature 444, 267 – 269 (2006)

[2] *Environmental colloids and particles*, IUPAC series on analytical and physical chemistry of environmental systems, K.J. Wilkinson, J.R. Lead (eds.), Wiley Interscience 2007

[3] *Aqueous suspensions of carbon nanotubes: surface oxidation, colloidal stability and uranium sorption*, A. Schierz[1], H. Zänker, Environmental Pollution 157, 1088 – 1094 (2009)

Project partners
· University of South Carolina, USA[1]
· Universität Göttingen, Germany
· Universität Wien, Austria

hypothetical release to the environment. Various methods were used to characterize the properties of the pristine and the treated material. Furthermore, colloidal stability of CNTs in aqueous solution was investigated. In Fig. 1 the temporal development of the scattered light intensity (a measure of CNT concentration) of the suspensions after ultrasonication is presented. It shows that the scattered light intensity decreased from 1,100 to about 30 cps within 24 hours for the pristine CNTs. Simultaneously, a deposition of black flocks became visible at the bottom of the sample cell. Hence, pristine CNTs do

not form stable colloids. By contrast, the scattered light intensity of the suspended modified CNTs remained nearly constant over a period of more than 14 days (decrease only ~ 25 %), i.e. this colloidal suspension proved to be stable. This is due to the generation of deprotonable carboxylic groups (COOH groups) on the CNT surface during surface oxidation (these groups could also be detected by infrared spectroscopy). Furthermore, the figure demonstrates that also humic acid, which is ubiquitous in environmental waters, is able to stabilize CNTs as colloids since it acts as a natural surfactant.

Interaction of actinides
with isolated bacterial cell wall components

Astrid Barkleit, Henry Moll

Bacteria are very important for the bio-remediation of the environment because they are able to adsorb radionuclides and other heavy metals. They significantly influence mobilization and immobilization of metal ions in the soil. In order to better understand the interaction of heavy metals with the biosphere, knowledge of the binding mechanisms on the molecular level is essential. The main binding sites of bacterial cell surfaces for heavy metal ions are phosphoryl, carboxyl, hydroxyl, and amino groups. We investigate the interaction of various actinides with isolated cell wall compartments, which are assembled like puzzle pieces and are thus able to recognize complex biological systems.

Bacteria can be differentiated into two large groups based on the chemical and physical properties of their cell walls. Gram-positive bacteria have a thick multilayered peptidoglycan envelope, which amounts to up to 50 % of the dry mass of the cell wall. Gram-negative bacteria only have a thin monolayered peptidoglycan envelope (Fig. 1). Peptidoglycan consists of chains of sugar molecules (polysaccharides = glycan) which are cross-linked with amino acid strings (peptides). The most important compartment of the cell envelope of Gram-negative bacteria is lipopolysaccharide. It is embedded in the outer membrane of the microbe, sticking out into the environment. Lipopolysaccharide plays a key role in the protection against contaminants and selective assimilation of needed small molecules or metals. It accounts for about 30 % of the whole cell wall of Gram-negative bacteria. Whereas lipopolysaccharide contains an especially high amount of phosphoryl groups for
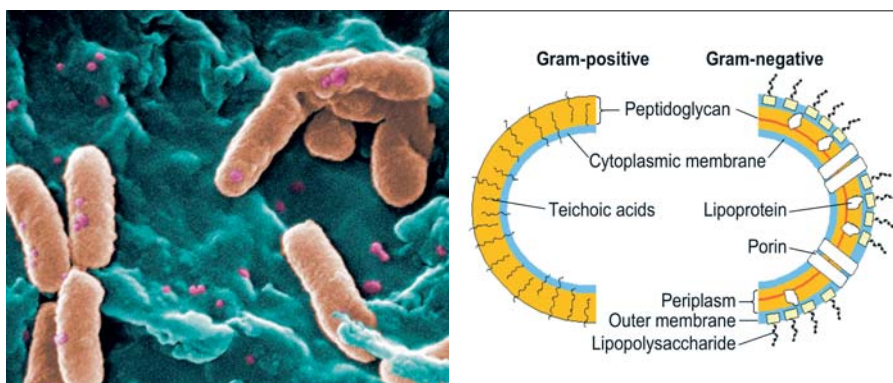

Fig. 1: Left: Gram-negative bacteria *Pseudomonas aeruginosa* (scanning electron micrograph (SEM); source: http://commons.wikimedia.org; photo: CDC/ Janice Haney Carr).
Right: Scheme of bacterial cell walls of Gram-positive and Gram-negative bacteria.

metal binding, they are missing in peptidoglycan.

We investigated the interaction processes of isolated lipopolysaccharide biomacromolecules from *Pseudomonas aeruginosa* and peptidoglycan biomacromolecules from *Bacillus subtilis* with uranium(VI) and curium(III). Uranium is widely spread in the environment due to uranium mining and milling, or applications in industry. Curium, a solely man-made actinide, is highly radiotoxic and very hazardous once it has been released, for instance from nuclear waste repositories. Both actinides show excellent luminescence properties. Hence, we could study their interactions with the biomacromolecules with time-resolved laser-induced fluorescence spectroscopy (TRLFS) over a wide pH range using trace concentrations. Additionally, potentiometric titrations were carried out to determine the deprotonation constants of the biomacromolecules and stability constants of the respective uranium complex species.

Fig. 2 depicts selected luminescence spectra of uranium and curium with

lipopolysaccharide at different pH values. The spectra of the uranium lipopolysaccharide system show a strong increase of the luminescence intensity with rising pH and lipopolysaccharide concentration, connected with a strong red shift of the peak maxima, compared to the free aquatic uranyl ion UO_2^{2+}(aq). This luminescence behavior is characteristic of the formation of very stable uranyl complexes with organic phosphoryl or inorganic phosphate groups [1]. Three different luminescence lifetimes over the measured pH range refer to three different phosphoryl coordinated uranyl lipopolysaccharide species. In combination with potentiometry, the composition and stoichiometries of these complexes could be identified. Additionally, a uranyl lipopolysaccharide species with carboxyl coordination could be determined with potentiometry only [2].

With increasing pH, the luminescence spectra of curium with lipopolysaccharide show a red shift of the peak maximum of the free aquatic curium ion Cm^{3+}(aq) with three domains of new peak maxima (Fig. 2) connected with three different lumines-

cence lifetimes, indicating the formation of three different curium lipopolysaccharide complex species. These luminescence properties could be assigned to a phosphoryl coordinated complex, a carboxyl coordinated species, and one with hydroxyl coordination.

Up to pH ~ 5.6 the luminescence spectra of the uranium peptidoglycan system show a slight increase of the luminescence intensity connected with a red shift of the peak maxima, and then again a strong decrease of the luminescence intensity caused by a quenching uranyl complex species. This inferior luminescence behavior is typically caused by the formation of uranyl carboxyl complexes. Two different luminescence lifetimes could be detected, referring to two luminescent complexes. Again, we could identify the uranyl peptidoglycan species in combin-

ation with potentiometry. We found two carboxyl coordinated complexes with different stoichiometries, and the quenching species was identified as a complex with carboxyl coordination and an additional coordination through a hydroxyl or amino group [3].

Likewise, the luminescence spectra of the curium peptidoglycan system show a red shift of the peak maximum to only one new maximum, connected with also only one new luminescence lifetime which belongs to the sole curium peptidoglycan complex species with carboxyl coordination.

The speciation of the various uranium(VI) and curium(III) complexes with lipopolysaccharide and peptidoglycan biomacromolecules (Fig. 3) could be calculated with the stability constants determined with potentiometry and time-resolved laser-induced fluorescence spectroscopy. The comparison of the complexation of uranium and curium with lipopolysaccharide and peptidoglycan shows that uranium has a stronger tendency to bind with phosphoryl groups than curium. Uranium forms stable complexes with carboxyl or other functional groups only in absence of phosphoryl groups and only in the middle pH range (Fig. 3, U-PGN system) whereas curium forms similarly stable complexes with carboxyl, phosphoryl, and hydroxyl groups over a wide pH range (Fig. 3, Cm-LPS system). In general, lipopolysaccharide seems to have a better binding potential for metal ions over a wider pH range than peptidoglycan.
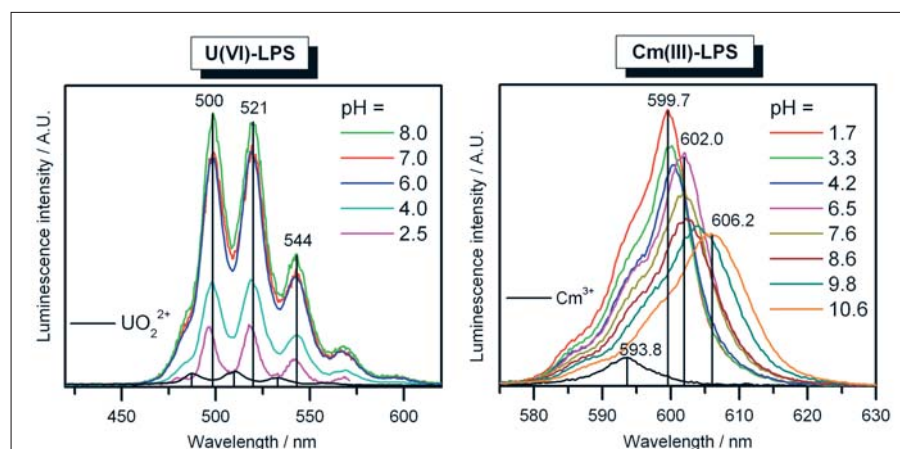

Fig. 2: Samples of luminescence spectra of uranium and curium with lipopolysaccharide (LPS) at different pH values.
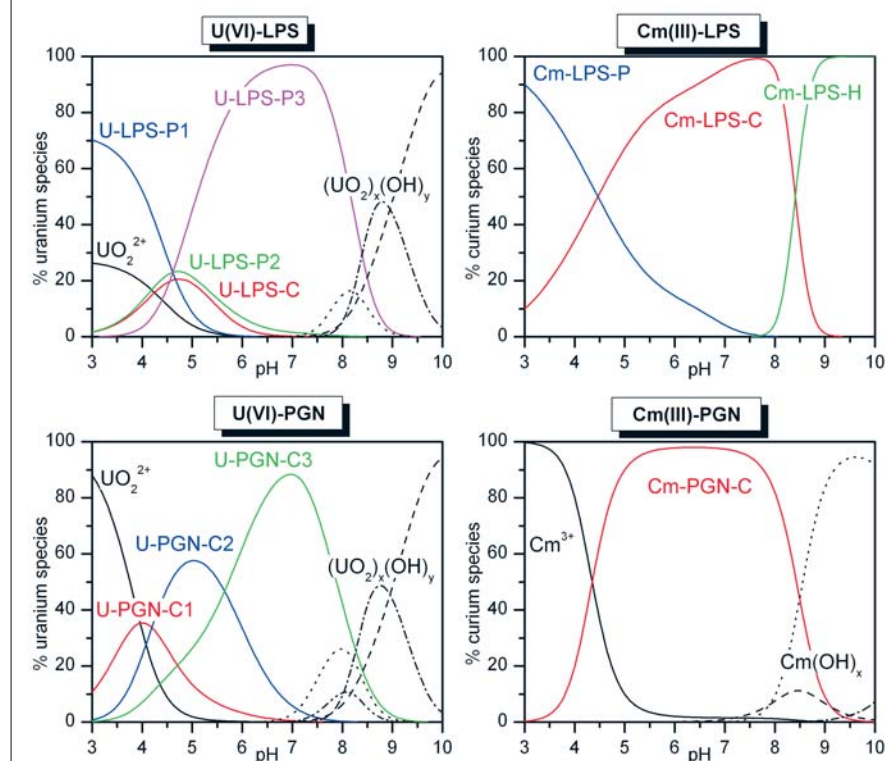

Fig. 3: Speciation of the different uranyl and curium lipopolysaccharide (LPS) and peptidoglycan (PGN) species in aquatic solution. P = Phosphoryl coordination. C = Carboxyl coordination. H = Hydroxyl coordination.

References

[1] *Uranium(VI) complexes with phospholipid model compounds – A laser spectroscopic study*, A. Koban, G. Bernhard, Journal of Inorganic Biochemistry 101, 750 – 757 (2007)

[2] *Interaction of uranium(VI) with lipopolysaccharide*, A. Barkleit, H. Moll, G. Bernhard, Dalton Transactions, 2879 – 2886 (2008)

[3] *Complexation of uranium(VI) with peptidoglycan*, A. Barkleit, H. Moll, G. Bernhard, Dalton Transactions, submitted (2008)

Humic substances and their influence
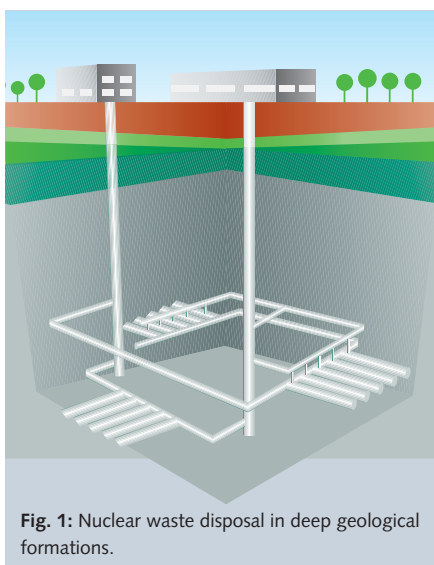## on the mobility of actinides in clay formations

Fig. 1: Nuclear waste disposal in deep geological formations.

Susanne Sachs, Katja Schmeide,
Adéla Křepelová

The main objective of a final repository for highly radioactive nuclear waste is to protect people and the environment from the risks caused by the waste. According to waste management concepts, the radioactive waste should finally be stored in deep geological formations (Fig. 1). In order to keep the waste safe in the long run and to isolate it from the biosphere, a multi-barrier system consisting of geological and technical barriers has to be used.

All over the world, scientists are studying whether different rock formations, mainly salt, argillaceous and crystalline rocks, e.g. granite, are acceptable as nuclear waste repositories. In Germany, all three of these types of rock formations come into consideration [1]. A comprehensive database on the properties of salt rock and salt formations relevant for the storage of highly radioactive nuclear waste is already available. However, for granite and clay formations further studies are still necessary to be able to compare whether different rock formations are suitable as a host rock.

Radionuclides with long radioactive half-lives, such as actinides as well as technetium-99, iodine-129, and selenium-79, play a prominent role for the safety case of a nuclear waste repository. In order to assess whether these radionuclides are mobile in the surroundings of a nuclear waste repository in case of an accident scenario, fundamental knowledge about all conceivable geochemical processes is a prerequisite. Our studies, which were funded by the German Federal Ministry of Economics and Technology and by the European Commission within the integrated project FUNMIG, contribute to this understanding.

The migration behavior of actinides in an aquifer can strongly be affected by humic substances (humin, humic and fulvic acids), organic macromolecules ubiquitously found in natural environments. Due to their solubility in the pH range of natural waters, their ability to form complexes and colloids as well as their redox properties, humic and fulvic acids can influence both the immobilization and transport of actinides. Most natural clays are closely associated with natural organic matter, e.g. humic acid- and fulvic acid-like compounds, which can be mobilized from clay. Both organic compounds associated with clay and organic compounds released from clay can influence the mobility of metal ions such as actinides.

In order to determine the influence of humic acid on the mobility of actinides in clay formations, we studied the sorption of Am(III), Np(V) and U(VI) onto kaolinite, which is representative of clay minerals. These actinides were selected as examples of actinides in different oxidation states.

The sorption experiments showed that humic acid sorption onto kaolinite decreases with increasing pH value [2]. The sorption of actinides onto kaolinite was found to be influenced by pH, ionic strength, presence of CO_2, actinide concentration and humic acid presence. Fig. 2 shows the sorption of Am(III), Np(V) and U(VI) onto kaolinite in absence or presence of humic acid. As can be seen from Fig. 2a, the Am(III) sorption onto kaolinite is very strong over the entire pH range and is only slightly influenced by humic acid. In contrast, the Np(V) sorption onto kaolinite (Fig. 2b) is much lower. It increases with pH up to pH 8.5 and decreases again at higher pH values. In presence of humic acid, the Np(V) uptake is further decreased between pH 7.5 and pH 10.5. The U(VI) sorption onto kaolinite (Fig. 2c) shows a broad maximum between pH 5.5 and pH 8. Humic acid enhances the amount of adsorbed U(VI) in the acidic pH range and reduces the U(VI) sorption in the near-neutral pH range compared to the system without humic acid.

These results show that humic substances are able to influence the sorption of actinides onto kaolinite, and, thus, their mobility. The increase of the actinide sorption in the acidic pH range compared to the system without humic acid can be attributed to the humic acid sorption onto the mineral, a scenario leading to additional binding sites for actinides. Fig. 3 shows a scheme for the sorption of metal ions and humic substances onto clay
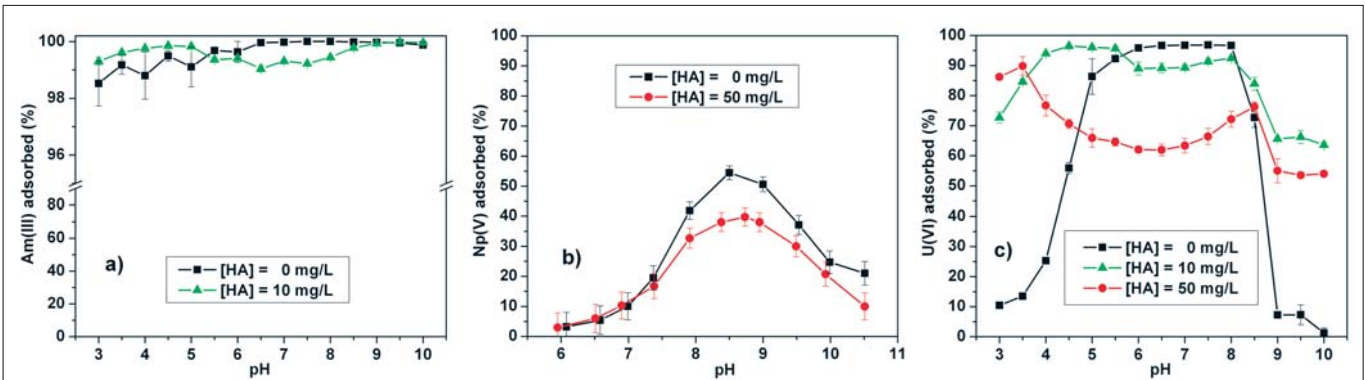
Fig. 2: (a): Am(III), (b): Np(V), and (c): U(VI) sorption onto kaolinite in absence and presence of humic acid (HA). Experiments were performed under ambient atmosphere with initial Am(III), Np(V) and U(VI) concentrations of $1 \cdot 10^{-6}$ M, a solid-to-liquid-ratio of 4 g kaolinite/L and an ionic strength of 0.01 M NaClO$_4$.

minerals. The reduction of the actinide sorption in the near-neutral pH range can be attributed to the formation of aqueous actinide humate complexes. The comparison of the actinide sorption behavior shows that the sorption of actinides depends strongly on their oxidation state and, thus, their speciation. In case of U(VI), the species sorbed onto kaolinite in the absence and presence of humic acid were identified by time-resolved laser-induced fluorescence spectroscopy [3] and by extended X-ray absorption fine structure spectroscopy [4]. These structural data are an important basis for modeling the U(VI) sorption onto kaolinite.

The studies described above used an isolated humic acid and a pure clay mineral. However, natural clays comprise a mix of organic matter. Therefore, more complex interactions are expected. In order to approach natural conditions and to identify effects of humic substances associated with natural clays which influence the sorption behavior of metal ions, we developed an artificial humic substance-kaolinite-associate (HSKA) as model substance and studied the sorption of U(VI) onto this product [5]. It was found that the humic matter associated with kaolinite also exhibits an immobilizing as well as a mobilizing effect on U(VI). However, due to structural and functional dissimilarities of the humic substances, the U(VI) sorption onto the synthetic HSKA differs from that of U(VI) in the system U(VI)/humic acid/kaolinite with separately added pure humic acid. Thus, it was concluded that natural humic substances associated with clay or free in solution can show different mobilizing effects on metal ions.

The present results are going to be compared to those for natural organic matter-containing clays, which we are currently studying. In order to imitate natural conditions more closely, diffusion experiments are performed to study the influence of humic substances on the actinide migration in compacted clay.

References

[1] *Endlagerung radioaktiver Abfälle in Deutschland. Untersuchung und Bewertung von Regionen mit potenziell geeigneten Wirtsformationen*, BGR, Hannover/Berlin, 2007

[2] *Uranium(VI) sorption onto kaolinite in the presence and absence of humic acid*, A. Křepelová, S. Sachs, G. Bernhard, Radiochimica Acta 94, 825 – 833 (2006)

[3] *U(VI)-kaolinite surface complexation in absence and presence of humic acid studied by TRLFS*, A. Křepelová, V. Brendler, S. Sachs, N. Baumann, G. Bernhard, Environmental Science & Technology 41, 6142 – 6147 (2007)

[4] *Structural characterization of U(VI) surface complexes on kaolinite in the presence of humic acid using EXAFS spectroscopy*, A. Křepelová, T. Reich[1], S. Sachs, J. Drebert[1], G. Bernhard, Journal of Colloid and Interface Science 319, 40 – 47 (2008)

[5] *Sorption of U(VI) onto an artificial humic substance-kaolinite-associate*, S. Sachs, G. Bernhard, Chemosphere 72, 1441 – 1447 (2008)

Project partner

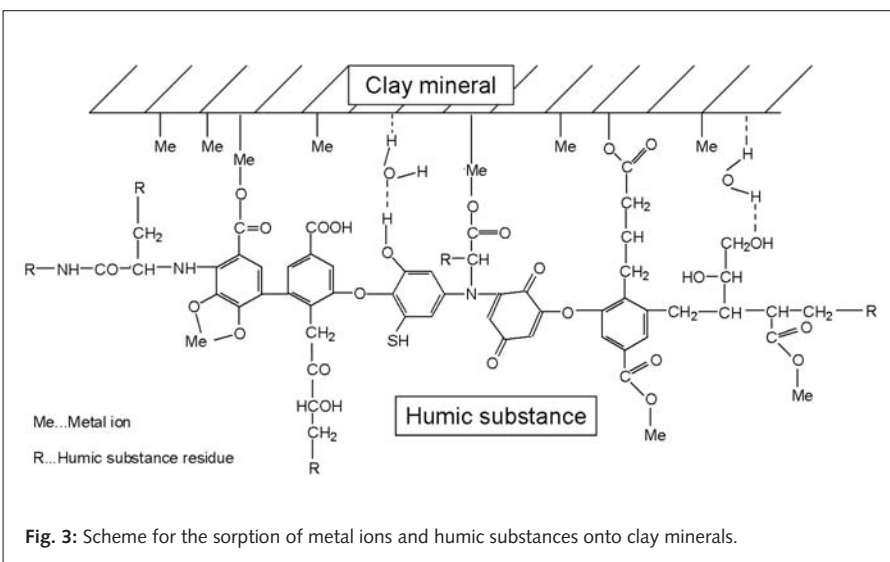· Institute of Nuclear Chemistry, Johannes Gutenberg Universität Mainz, Germany[1]

Fig. 3: Scheme for the sorption of metal ions and humic substances onto clay minerals.

Mobilization of actinides
through bioligands secreted by microbes

Henry Moll, Gert Bernhard

Today, various human activities are responsible for the contamination of shallow and deep groundwater by actinides. These activities include the injection of low- and intermediate-level radioactive waste into deep geological formations, underground atomic bomb testing, leaching from mine waste, and accidental leakage from current and future underground radioactive waste repositories. The interaction between microbes and hazardous actinides may influence their environmental migration behavior once they have been released.

Microorganisms can interact with actinides through both direct and indirect pathways (Fig. 1). This study, which was partly funded by the German Federal Ministry of Economics and Technology, focuses on an investigation of indirect processes between microbes and actinides. Indirect processes include the formation of soluble complexes of actinides with various bioligands secreted by the resident microorganisms.

Microbes like Pseudomonads are ubiquitous soil and ground water bacteria. In our institute, we were able to isolate and identify these microbes in uranium waste piles or sewage from uranium mill tailings where they are able to live under harsh environmental conditions. In environments poor in iron, the fluorescent *Pseudomonas* species secrete bioligands, the so-called pyoverdins. Due to their unique structure, pyoverdins have a great potential to bind metals. The functional groups that are responsible for binding the metals are the catechol group of the chromophore and two ligand sites in the peptide chain, i.e. one or two hydroxamate groups and one or two α-hydroxy acid moieties (Fig. 1). In this report, we present results describing the complexation between the hazardous actinide elements uranium and curium and the pyoverdins released by *Pseudomonas*

Fig. 1: Direct (A-C) and indirect (D) interaction processes of microbes with released actinides. The bioligands investigated here, the pyoverdins, are highlighted. Asterisks indicate the complexation sites involved in metal binding.
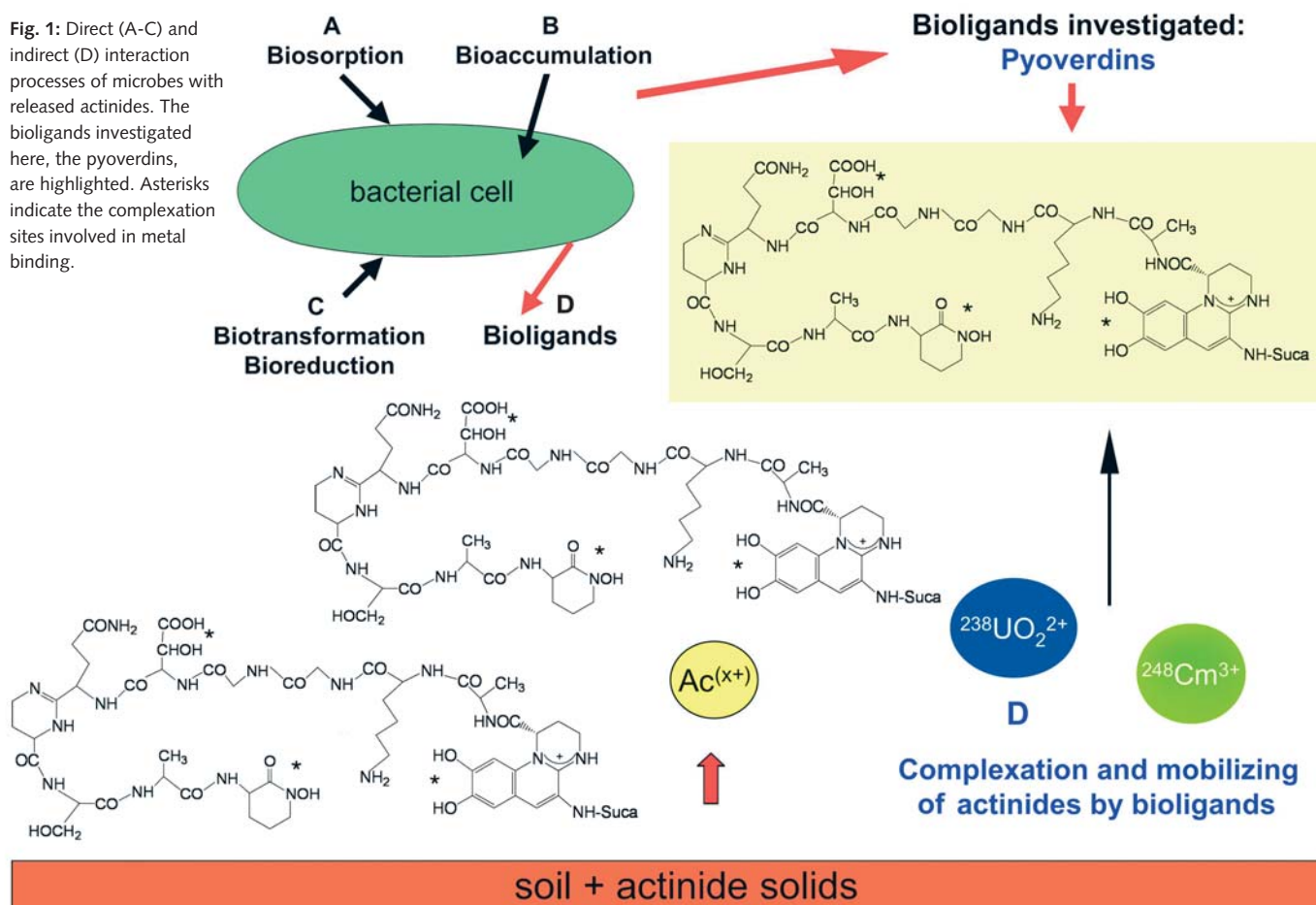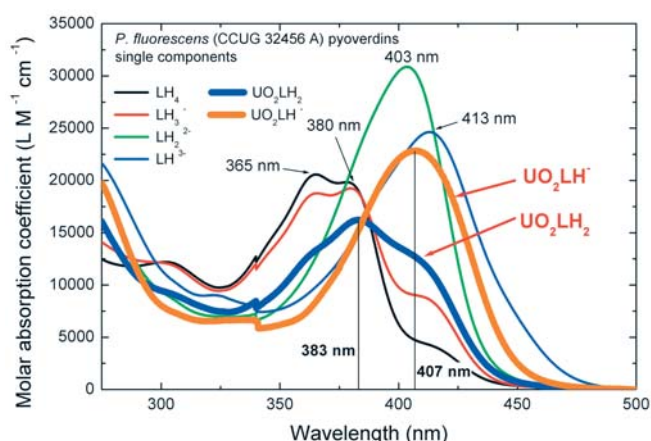
Fig. 2: Absorption spectra of the individual components of the aqueous P. fluorescens (CCUG 32456) pyoverdin system with and without UO_2^{2+}. L^{4-} = deprotonated pyoverdin molecule.
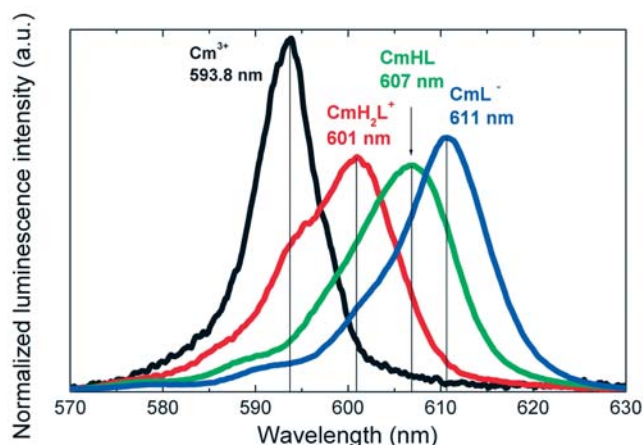

Fig. 3: Luminescence emission spectra of the aqueous Cm^{3+}-P. fluorescens (CCUG 32456) pyoverdin species. The spectra are scaled to the same peak area. L^{4-} = deprotonated pyoverdin molecule.

fluorescens (CCUG 32456) cells isolated from the granitic rock aquifers at the Äspö hard rock laboratory (HRL) in Sweden [1, 2]. This study is part of an international cooperation between the Institute of Radiochemistry at the FZD and the Göteborg University (Department of Cell and Molecular Biology, Microbiology) in Sweden. In this paper, we are able to answer the following question: besides iron(III), do pyoverdins also form strong species with hazardous and radiotoxic actinides? If the answer to our question is yes, it would have a serious impact on the amount of actinides that can leach out of a nuclear waste disposal site.

Both the actinides (UO_2^{2+}, Cm^{3+}) and the pyoverdins have excellent properties for direct speciation studies with spectroscopic techniques. Ultra-violet and visible-light (UV-vis) spectroscopy, as well as time-resolved laser-induced fluorescence spectroscopy with ultrafast pulses (fs-TRLFS) in combination with a factor analysis based data evaluation procedure, provides a practicable method for investigating the speciation of UO_2^{2+} in the aqueous P. fluorescens (CCUG 32456) pyoverdin system. In our study, the pyoverdin molecule is denoted LH_4 according to the general assumption that pyoverdin molecules can liberate four labile protons from the complexing sites most likely responsible for metal binding. Four different pyoverdin species, i.e. LH_4, LH_3^-, LH_2^{2-}, LH^{3-}, and two uranyl pyoverdin complexes, i.e. UO_2LH_2 and UO_2LH^-, could be identified by their individual absorption

spectra (Fig. 2). The identified uranium-pyoverdin complexes dominate the uranium speciation in the environmentally relevant pH range between 4 and 8 [1]. The formation of the uranyl pyoverdin complexes results in a static fluorescence quenching and, as a consequence, in drastic changes of the fluorescence properties of pyoverdin. Therefore, pyoverdins could be used as fluorescence probes to investigate siderophore-mediated processes, e.g. to measure the uptake of metals by bacterial cells, in biological systems. The results of this study indicate that pyoverdins present in groundwater at the µM concentration level can contribute to the increased dissolution of uranium from, for example, mine waste. At the Rossendorf Beamline (ROBL) at the ESRF, we investigated the structure of uranium-pyoverdin complexes in aqueous solution, by using extended X-ray absorption fine structure (EXAFS) spectroscopy. The results indicate a strong affinity of uranyl to the catechol functionality of the pyoverdin molecule.

The unknown interaction between soluble species of curium(III) and pyoverdins was studied at trace curium(III) concentrations (3×10^{-7} M) using time-resolved laser-induced fluorescence spectroscopy (TRLFS). Strong Cm^{3+} pyoverdin species are formed, indicating that these unique bioligands have a great potential to mobilize curium(III) in the biologically relevant pH range [2]. Three Cm^{3+} pyoverdin complexes, CmH_2L^+, $CmHL$, and CmL^-, could be identified by their individual emission spectra (Fig. 3). We

were able to observe an indirect excitation mechanism for the curium(III) luminescence in the presence of pyoverdin molecules.

In conclusion, both actinides form strong soluble pyoverdin species in aqueous solutions. The chemical reactions between both actinides (UO_2^{2+}, Cm^{3+}) and aqueous pyoverdin species were determined using different spectroscopic techniques. The stability constants of these individual reactions can be used directly in safety calculations to quantify the actinide-mobilizing effect of the pyoverdins released, for example, in the vicinity of a nuclear waste repository. Such complexation studies of selected bioligands are essential to explain the overall interaction processes of actinides with microbes at the molecular level.

References

[1] Characterization of pyoverdins secreted by a subsurface strain of Pseudomonas fluorescens and their interactions with uranium(VI), H. Moll, M. Glorius, G. Bernhard, A. Johnsson, K. Pedersen, M. Schäfer, H. Budzikiewicz, Geomicrobiology Journal 25, 157 – 166 (2008)

[2] Curium(III) complexation with pyoverdins secreted by a groundwater strain of Pseudomonas fluorescens, H. Moll, A. Johnsson, M. Schäfer, K. Pedersen, H. Budzikiewicz, G. Bernhard, BioMetals 21, 219 – 228 (2008)

Project partner
· Department of Cell and Molecular Biology, Microbiology, Göteborg University, Sweden

The Forschungszentrum Dresden-Rossendorf (FZD) is a multi-disciplinary research center for natural sciences and technology. It is the largest institute of the Leibniz Association and is equally funded by the Federal Republic of Germany and the Federal States, in particular by the Free State of Saxony. At the FZD, around 330 scientists are engaged in three different research programs of basic and application-oriented research. Scientists working in the Advanced Materials Research program investigate the reactions of matter in strong fields and at small dimensions. Research and development in the Cancer Research program is focused on the imaging of tumors and the effective radiation treatment of cancer. How can humankind and the environment be protected from technical risks? – This question is in the center of research in the Nuclear Safety Research program of the FZD.

In the following Facts & Figures section data presenting the scientific output in the Nuclear Safety Research program are given as well as information on staff and funding at the FZD.

Facts & Figures

Scientific staff – Nuclear safety research

staff scientists
third-party funded scientists
guest scientists
postdocs
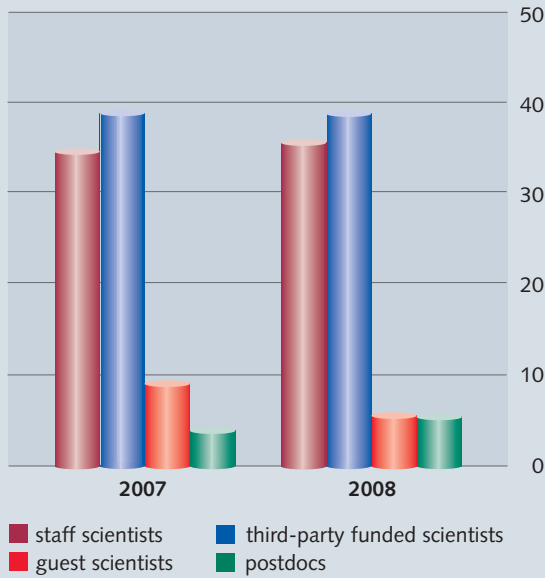
Distribution of positions occupied by scientific personnel in the Nuclear Safety Research program of the FZD. Third-party funded scientists, guest scientists, and postdocs represented by the corresponding figures are given in units of paid full-time posts.*

Budget	2007		2008	
Research Programs	Core Funding T€	Third-Party Funding T€	Core Funding T€	Third-Party Funding T€
Advanced Materials Research	19.776	1.600	17.822	4.622
Cancer Research	7.729	1.141	9.340	840
Nuclear Safety Research	**12.577**	**5.086**	**13.069**	**3.660**
Large-Scale Facilities	14.564	1.487	18.401	4.028
Sum	54.646	9.314	58.632	13.150

Share of each research program, as well as of the experimental facilities located at the FZD, of both core and third-party funding during the last two years.
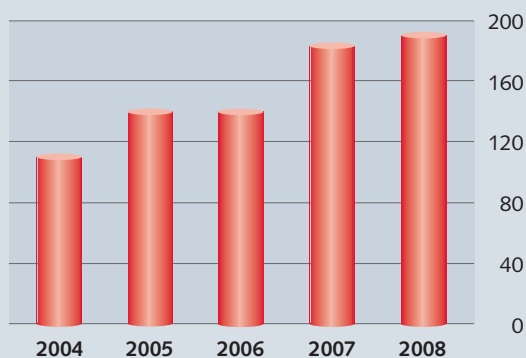
Patents – FZD

Advanced Materials Research
Cancer Research
Nuclear Safety Research
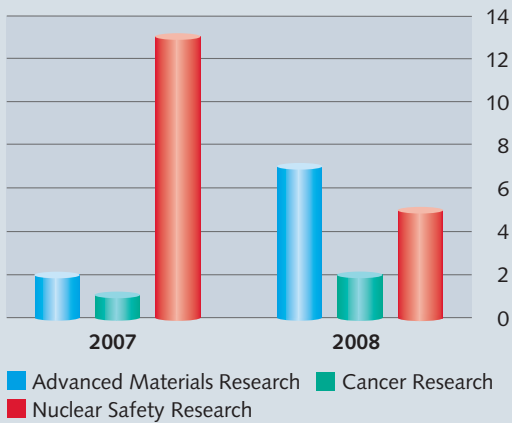
Number of applications for a patent filed in each research program of the FZD in 2007 and 2008.
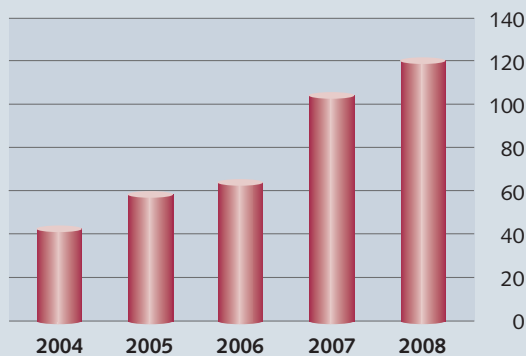
*All figures as of 1st March 2009.
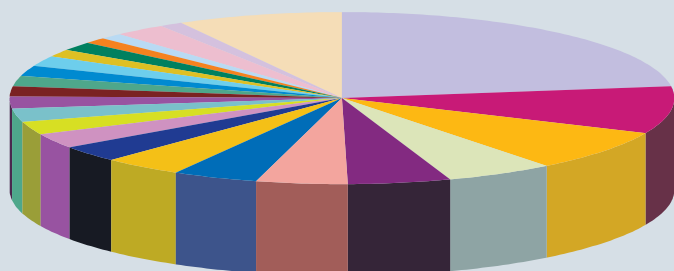
Publications – Nuclear safety research

Number of peer-reviewed articles by scientists from the FZD's Nuclear Safety Research program. The figures include reviewed proceedings (2004: 39, 2005: 50, 2006: 53, 2007: 64, 2008: 71).

Doctoral students – FZD

Growth in number of doctoral students at the FZD from 2004 until 2008.

International guest scientists – FZD

Distribution of the international guest scientists who visited the FZD for the purpose of research between 2007 and 2008 according to their countries of origin.

Russia	59	USA	11	Japan	6	Latvia	4
Czech Republic	23	Bulgaria	10	Turkey	6	Portugal	4
Poland	20	China	8	France	5	Algeria	3
Ukraine	14	Australia	7	Netherlands	5	Egypt	3
India	13	Italy	7	Romania	5	Israel	3
Hungary	11	Great Britain	6	Spain	5	others	21

Organizational Chart

	General Assembly

Supervisory Board
Chairman: Dr. Gerd Uhlmann
Deputy: Dr. Jan Grapentin

Scientific Advisory Board	**Board of Directors**	**Works Committee**
Chair: Prof. August Schubiger	Scientific Director Administrative Director	Chair: Siegfried Dienel
	Prof. Roland Sauerbrey Prof. Peter Joehnk	

Scientific Technical Council
Chair: Prof. Joachim Wosnitza

Support Staff

ADVANCED MATERIALS RESEARCH

Dresden High Magnetic Field Laboratory	Institute of **Ion Beam Physics and Materials Research**	**Research Technology**
Prof. Joachim Wosnitza	Prof. W. Möller and Prof. M. Helm	Dr. Frank Herbrand

CANCER RESEARCH

Institute of **Radiopharmacy**	Institute of **Radiation Physics**	**Technical Service**
Prof. Jörg Steinbach	Prof. Thomas Cowan	Dr. Wolfgang Matz

NUCLEAR SAFETY RESEARCH

Institute of **Safety Research**	Institute of **Radiochemistry**	**Administration**
Prof. Frank-Peter Weiß	Prof. Gert Bernhard	Andrea Runow

■ Advanced Materials Research   ■ Cancer Research   ■ Nuclear Safety Research

March 2009